AD NUMBER
AD337920
CLASSIFICATION CHANGES
TO: unclassified
FROM: confidential
LIMITATION CHANGES
TO: Approved for public release, distribution unlimited
FROM: Controlling DoD Organization. Defense Threat Reduction Agency, 8725 John J. Kingman Road, Fort Belvoir, VA 22060-6201.
AUTHORITY
DTRA ltr, 12 Jul 2006; DTRA ltr, 12 Jul 2006

FORCE project RAND

RESEARCH MEMORANDUM

The RAND Corporation
SANTA MONICA • CALIFORNIA

(4) NA (5) 739200 (7) NA (8) LW

AFSWP 1134

CONFIDENTIAL
FORMERLY RESTRICTED DATA

Handle As Restricted Data In Foreign Dissemination
Section 144b, Atomic Energy Act, 1954

(9) NA

JAN 18 1960

U. S. AIR FORCE

PROJECT RAND

RESEARCH MEMORANDUM

(6) SUMMARY REPORT OF RAND WORK ON THE AFSWP FALLOUT PROJECT, (U)

(10) R. R. Rapp.

(11) February 25, 1959

Copy No. 32

(12) 68p.
(13) NA
(14) Rept. no. RM-2334
(15)-(17) NA
(18) DASA
(19) 1134
(20) C-FRD
(21) NA

Assigned to _____

This is a working paper. Because it may be expanded, modified, or withdrawn at any time, permission to quote or reproduce must be obtained from RAND. The views, conclusions, and recommendations expressed herein do not necessarily reflect the official views or policies of the United States Air Force.

DISTRIBUTION RESTRICTIONS

No restrictions on further distribution, other than those imposed by security regulations.

The RAND Corporation
1700 MAIN ST. • SANTA MONICA • CALIFORNIA

CONFIDENTIAL

SUMMARY

This report is a summary of the work done at The RAND Corporation on the radioactive fallout program of the Armed Forces Special Weapons Project. It discusses the best fit to the parameters which enter into the computation of radioactive fallout and the sensitivity of the final pattern to changes in these parameters. It is concluded that fallout forecasts can be made which, though not extremely accurate, can be of great value in operational problems.

RM-2334
2-25-59

CONTENTS

I. INTRODUCTION

A recent RAND report, Close-In Fallout,[1] presents a general survey of the basic mechanisms for understanding local fallout, which have been studied in great detail. Since the publication of this report, work has been in progress toward establishing a better definition of the problem presented by these basic mechanisms and improving our understanding of the details involved. The purpose of this paper is to present the results of studies made since the publication of Close-In Fallout and to bring out some slight changes in the concept of the fallout process. However, in order to provide a complete picture, a certain amount of the earlier background will be given, including a brief resume of the physical process of fallout and a definition of the problem. Following this, each of the parameters which enter into the problem will be taken up in detail, and the results of studies made over the past 18 months will be presented. The presentation will be of a conceptual nature rather than a mathematical formulation.

Because of the great amount of technical detail to be presented in this report, the scope of the subject matter will be more limited than in Ref. 1. The basic parameters for a surface-burst bomb will be discussed thoroughly, but the effect of height above the surface and of changing surface conditions can be only briefly touched upon. The extent to which local fallout can be determined will be considered, and the prospects for numerical forecasting will be presented. Since this is to be a report on research done at RAND, it cannot be considered as a general survey or status report on the entire problem of fallout. The work of the many other organizations engaged in fallout research has been used, but no comprehensive

summary has been made. This report, then, is a summary of the physical processes and mathematical models of local fallout from surface-burst atomic bombs. There is no biological, and only a minimum of radiological, information contained herein.

The detonation of an atomic device releases large amounts of energy either through the fission of heavy atoms or the fusion of light ones. The release of energy may be accomplished through fission only or through a combination of fission and fusion. The fragments of the fission of the heavy atoms are generally radioactive particles. Another source of radioactive particles or atoms is the activity induced in some types of stable atoms by the capture of neutrons. The nature of the radioactive products therefore varies greatly, depending on the mixture of fission and fusion in the bomb and the elements which are available nearby to capture neutrons. Because of the variation which is possible in the nature of the radioactive products, this report will not deal with any purely radiological parameters; instead, the fraction of the device will be the primary independent variable. The fractions which are used and which will be discussed further in this report are based on measurements of Molybdenum^{99} (Mo^{99}), a radioactive element formed in a predictable way by fission, which generally falls out without fractionation* and represents a very good measure of the radioactive fraction of the device. If the details of the radiological components of the bomb and the soil are known, it is always possible to synthesize a proper radiological factor to be multiplied by the fraction of the device, hence generating either dose rate, integrated dosage, or any other measure of

*Fractionation is the separation of different isotopes due to differences in the nature of the radioactive precursors.

the radioactivity.

The radioactive isotopes which are formed are, for the most part, contained in an extremely hot mass of air and residual bomb debris. At the time of detonation most of these isotopes will exist in the form of a cloud of ions. As the cloud rises and cools the isotopes form into particles by attaching themselves to solid particles which are swept through the cloud, or by condensation into minute drops, or by a combination of both processes. Naturally, the most refractory materials will form into particles first and some of the less refractory materials later. Of course, the noble gases will not condense at all. We have no measurements of particle formation inside the fireball; thus, our knowledge of the actual method of formation of the particles is not complete. However, an examination of the resulting particles enables us to estimate the distribution of their mass and size. It has also been determined that some radioactive elements which have gaseous precursors do not form particles early enough in the process to be precipitated in the same way as some of the more refractory materials. Thus, the problem of the refractionation -- the atmospheric separation of some of the radioactive elements from the main body of the fallout -- must be borne in mind.*

The particles which are thus formed and the activity which they carry represent one of the necessary inputs to any fallout model. The information which we have about the size, mass, and fall rates of these radioactive particles and the distribution of the radioactivity with particle size has actually all been deduced from observations of the fallout pattern (the two

*Strontium 90 and cesium 137, two materials strongly fractionating seem to be deposited in a way that is different from that of Mo^{99}.

different ways in which these deductions have been made will be discussed in detail later). This distribution represents one of the important initial parameters, for it is necessary to know what fraction of the activity resides in particles of different sizes.

The tremendous energy released by a nuclear detonation over a small space and in a short time causes a large bubble of hot air. This hot, low-density air has a tendency to rise through the atmosphere. As it rises it does work against the atmosphere and in so doing is cooled. It has been observed that the outward gradient of temperature, in the hot bubble of air, causes the central portion to rise relative to the outside portion of the cloud. This causes an overturning of the cloud, and a toroidal or smoke ring circulation develops. Most of the particles of radioactive debris end up in the core of the smoke ring. This is an extremely stable circulation. Most of the radioactivity is carried aloft with the cloud, and only a small fraction escapes from the toroidal circulation to be left behind to form a wake or stem. The material thus carried upward forms the radioactive cloud.

When the energy which caused the cloud to rise has been dissipated by rising through and mixing with the atmosphere, the cloud arrives at a stabilization point, the height of which depends very markedly on the yield and, to some extent, on the conditions in the atmosphere. For the larger yields, the toroidal circulation continues for a while after stabilization, and this tends to expand the radius of the toroid; thus, as the cloud approaches its stabilization point, a continued horizontal expansion is noticed. At about five or six minutes after detonation, when the cloud has stabilized, the initial space distribution of the radioactivity is

established. It is in the form of a ring-shaped body of debris of particles of various sizes. In addition to this ring-shaped body there will be some trailing material down along the wake or stem of the cloud. The experiments during Operation Redwing, about which more will be said later, definitely show that there is a very small fraction of the debris contained in the stem of the cloud. The space distribution of the radioactivity represents another important parameter of the radioactive fallout. These same Redwing experiments demonstrate quite conclusively that the majority of the radioactive debris is in the lower portion of the visible cloud and that it is contained in a ring around a central portion which has relatively little debris.

After stabilization, the toroidal circulation rapidly decays, and the particles of debris fall from that elevation to the ground. The particles will attain some sort of terminal velocity and will, of course, be transported by the wind. If it is assumed that the vertical motion of the air is negligible in comparison with the fall rate of the particles, then the vertical velocities of the particles can be computed. Thus, the fall rate of the particles, which will be a function of the size, shape, height, and density of the particles, is an important and necessary component of the fallout analysis.

It can be shown that for the particles which comprise the majority of the fallout, the wind can be considered to transport them with the speed of the wind. That is to say, there is no appreciable lag in the particles following the wind flow. Suffice it to state here that the wind will carry the particles in the horizontal direction, and it is imperative to know where the wind is going to carry them.

There are several variations in the wind which must be considered. First of all, there are large shears of the horizontal wind in the vertical, and these should be accounted for. Furthermore, some of the particles take quite a bit of time to reach the ground, and during this time the wind patterns will change, so the time variation of the winds must be taken into account. Also, some of the particles are carried over great distances, so we need to take into account the variation of the wind in the horizontal. Thus, to be precise, the wind should be considered as a function of the space dimensions and time.

To summarize, then, in order to compute or predict fallout it is necessary to know the distribution of activity with particle size, the distribution of the activity in space at the time of stabilization, the fall velocity of the particles, and the wind structure. In the following sections these parameters will be considered in turn. They will be considered chiefly in connection with surface-burst bombs in the megaton range.

Finally, we shall attempt a synthesis of the individual parameters into the final fallout pattern. Note that there is no necessity in this work for discussing the radiological nature of the debris. We speak of the fraction of the device, and we compute this fraction on the basis of Mo^{99} -- one of the best known fallout components. Thus, the cleanliness of the weapon, the fission-fusion ratio, the nature of fission products, or induced activities, need not concern us in defining a fallout pattern. We will define the fraction of the device, and if there is any further information as to the nature of the radioactive material, this can be incorporated with the fraction-of-device numbers and all the customary radiological values deduced. Obviously, since we have not considered radiological parameters, we will not concern ourselves with the biological effects of radiation.

II. ACTIVITY-PARTICLE SIZE DISTRIBUTION

There have been quite a few attempts to deduce the distribution of radioactivity with particle size. One of the most usual methods of making this deduction is to plot the position of various sized particles from various elevations in the clouds according to their fall velocity and the winds, then to measure the ground activity at that point and to assign the fraction of activity as a function of particle size in accordance with the amount on the ground associated with that particle size. This was essentially the method used to determine the particle size and activity distribution for the Jangle surface shot as presented in RAND report R-265-AEC.(2) It is also the essence of the Weather Bureau procedure in determining the activity-size distribution for tower shots.

Another more direct method is to simply measure the activity on particles that have been sized after they have been collected. This is the method used by Krey(3) in analyzing the activity and particle size distribution from the collections on YAG-40 at the Zuni Redwing shot.

Figure 1 presents several sets of results that have been obtained in the past. The scales may be awkward, but they are ideal for containing all of the data. The ordinate is a logarithmic scale and the abscissa is the integral of the Gaussian error function. Thus, a straight line on this particular graph would represent a "normal distribution" in the logarithm of the particle size. The graph is cumulative so that the fraction of material on particles less than the size shown on the ordinate is read on the abscissa. The heavy solid line is the log normal curve which is fitted to the distribution taken from Ref. 2. The circles are points from the distribution in Ref. 2. It can be seen that most of the data, at least near

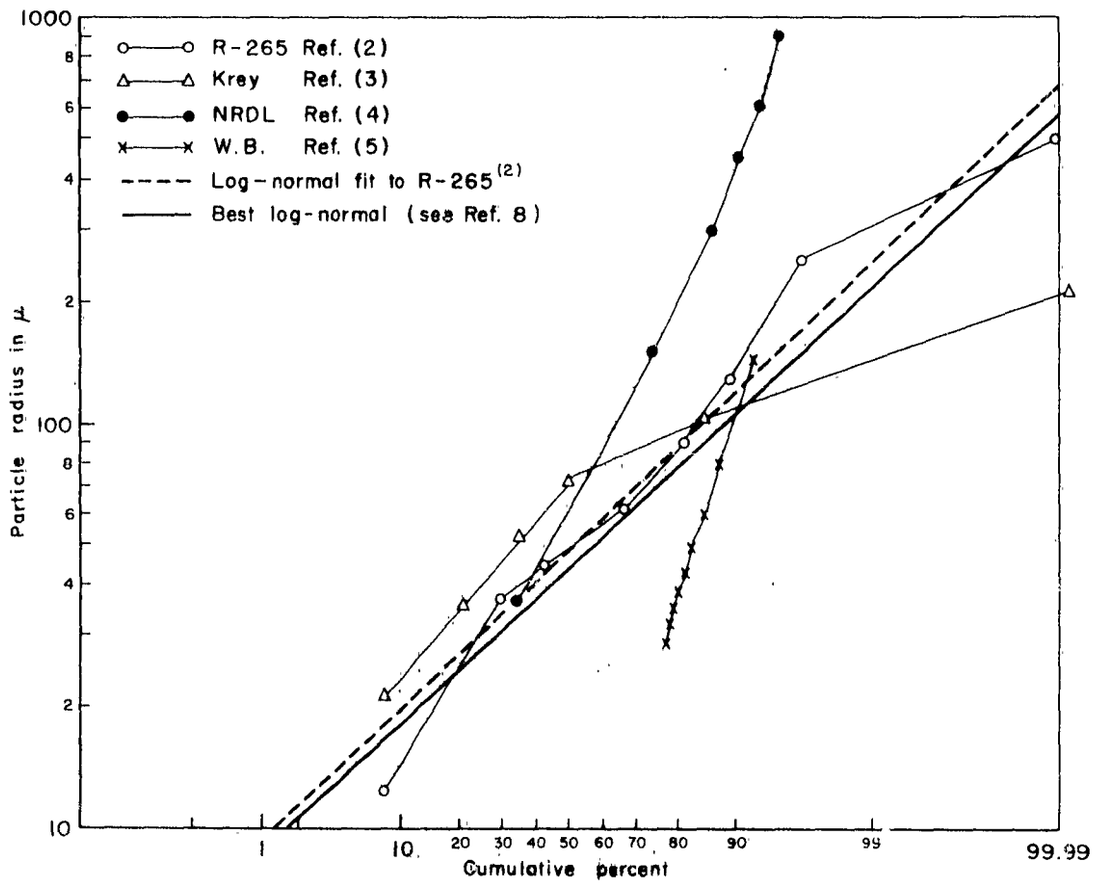

Fig. 1 — Some suggested particle size-activity distributions

the center of the graph, is clustered very closely around this line. It may perhaps be worthwhile to note some of the deviations from this. To the upper left of the straight line is shown the NRDL curve derived from Jangle surface and underground shots by analyzing particle size.(4) This shows a much larger fraction of large particles. It is believed that the fact that data from the underground shot were used in deriving this curve has caused it to indicate too many large particles for a surface burst. The short bit of curve on the lower right of the straight line represents the average of the Weather Bureau examination of the tower shots in Nevada.(5) It is to be expected that the tower shots would have a larger fraction of small particles because there is not as much dirt taken into the fireball.

The data from Krey's analysis of the collection on YAG-40 is interesting. The lower end of the curve, that is, the part dealing with the smaller sizes, shows an almost linear trend on the log-normal paper. However, for particles larger than 74 microns the curve falls off, showing 100 per cent of the material on particles less than 210 microns in radius. This is probably caused by the fact that the larger particles fall to earth long before they could reach the collection station. Thus, the curve representing Krey's data is based on a biased sample. The same may be true for the Ref. 2 curve which falls off in a similar manner but which reaches higher values.

A log-normal curve appears to be a good fit to the bulk of the data. The Weather Bureau curve for tower shots, which appears at the lower right of the surface-burst data, can be discounted because they are not surface bursts. The NRDL curve, at the upper left of the main body of data, can be discounted because of the inclusion of data from the underground shot.

The efficiency of large particles in Krey's curve and the estimate presented in Ref. 2 can be attributed to the removal of the large particles in such short time that they do not enter into the sampling procedures.

The manner in which the curves presented in Fig. 1 have been obtained is more or less biased. There has been no method found to date for getting a completely unbiased sample of the particle size from the original cloud and the prospect of obtaining unbiased measurements is not bright, because of the tremendous problems involved in sampling, sizing, and measuring the radioactive particles.

The work done to date has served to indicate that a log-normal distribution appears to be a reasonable choice for the distribution of activity with particle size. There has been some evidence that there is a different distribution of activity with particle size at different elevations; in other words, the distribution of activity with particle size is not independent of height. However, for the purposes of this study, the assumption was made that the activity distribution with particle size was completely independent of the activity distribution with height. A review of some of the attempts to separate the size distributions according to height indicates that the assumption of independence will not cause any serious difficulty. As a matter of fact, none of the observations are sufficiently accurate to warrant the conclusion of differing particle size-activity distributions with height.

Since the distribution appears to be a log-normal, and since the data studied so far has considerable bias, it was decided to attempt to reconstruct a log-normal particle size-activity distribution which would best fit the Zuni results on Operation Redwing. The basic assumptions of this

approach are that the distribution is log-normal, that it is independent of elevation (as mentioned above), that the distribution of activity with height is known, and that the winds are known as functions of space and time. The excellent series of weather maps which were analyzed by the Joint Task Force 7 Weather Group for the Redwing Tests[6] was used to construct time-varying and space-varying wind patterns. The distribution of the activity with height was taken from the rocket results as reported in "Fallout Studies During Operation Redwing."[7] Using the method of computation as outlined in Ref. 8, five different log-normal distributions* were chosen and each of them was used to make a computation of the activity at each of five different measuring stations. For each station a plot was made on axes which represented the mean of the logarithm of particle size for the ordinate and the standard deviation of the logarithm of particle size for the abscissa. Each of the five distributions on this graph are therefore represented by a point. At each of these five points the computed fraction of the device for that particular measuring station was entered. The five values of fractions were then used to subjectively construct lines of equal fraction of device as a function of mean of the logarithm of particle size and standard deviation of the logarithm of particle size. The measured value (see Ref. 9) was then used to find the line of possible means and standard deviations for

*The log-normal function is simply the Gaussian distribution in the logarithm of the variable. If $x = \log r$ and the distribution of x is normal, then

$$P(\log r) = \frac{1}{\sqrt{2\pi}\,\sigma_{\log r}} \; e^{-\frac{1}{2}\left(\frac{\log r - \overline{\log r}}{\sigma_{\log r}}\right)^2} \; d(\log r)$$

This is a two-parameter distribution in which the distribution is completely determined by the means of the logarithm of the particle radius and the standard deviation of the logarithm of the particle radius.

each of the stations. On Fig. 2 the observed range of each of the five stations is superimposed. It may be noted that there are no lines for the results from YAG-39. This station was at an extreme edge of the fallout pattern and the fallout did not arrive here until almost 24 hours after the event. With this long delay time the wind errors accumulate to such an extent that no confidence can be placed in the wind plot (see Sec. V). Therefore, lack of fit of this one station does not seriously discredit the results.

The other four stations show that the mean and standard deviation which best fit all of the stations must be within the area that has been chosen. Subjective best estimates for the mean of the logarithm of the radius and the standard deviation of the logarithm of the radius are 1.65 and 0.30 respectively. This particle size distribution was then used in the model with the wind from the Tewa shot from Operation Redwing. The results that this particle size-activity distribution gave on the independent test with the Tewa shot were most gratifying. A plot of the computed versus the measured fraction is shown in Fig. 3.

Because of the known uncertainty in the particle size distribution, it is necessary to know something about the effect of any changes in the distribution on the fallout pattern. It is apparent that a large fraction on small particles will produce an extensive pattern. A large fraction on large particles will produce a less extensive pattern but one of greater intensity. For a log-normal distribution with a given standard deviation, an increase in the mean will place more activity on larger particles which are deposited near ground zero and less on particles which are, for the most part, too small to appear in the local fallout in any event. Thus

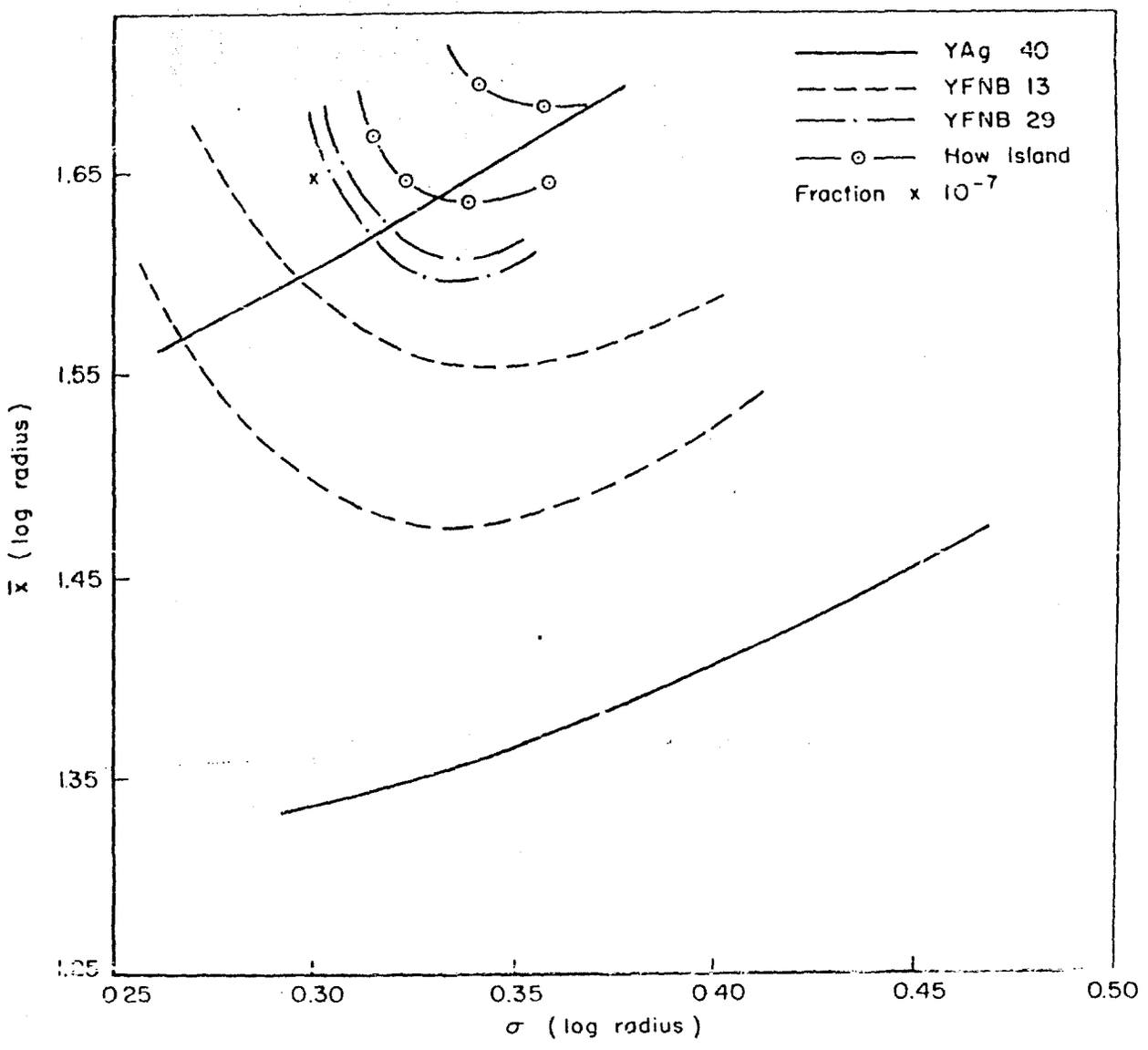

Fig. 2 — Subjectively determined combinations of $\overline{\log r}$ and $\sigma_{\log r}$ which would fit within the standard error of observation of fraction down at 4 observing stations

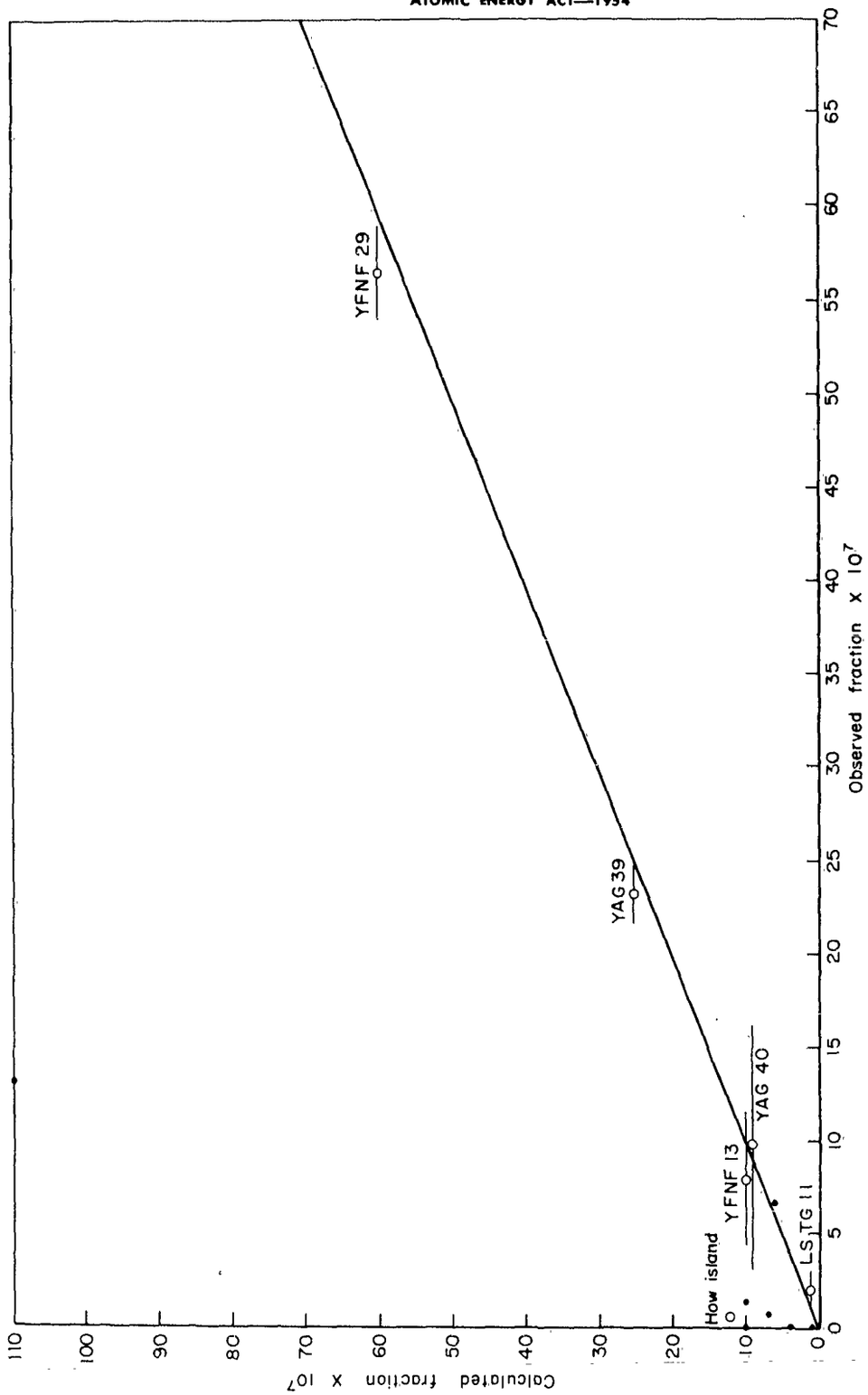

Fig. 3 — Calculated versus observed fraction of device per square kft for the Tewa shot—Operation Redwing

the changes in the value of the mean of the logarithm produce large changes in the pattern near ground zero. For example, a change in the mean of the log of r from 1.47 to 1.67 increased the fraction at the stations within 20 mi of ground zero by factors of from 4 to 10. At more distant stations, where particles from the center of the distribution cause the fallout, the shift of the mean will cause less change in the fraction in any particle size range, therefore a shift in the mean of the magnitude quoted above produces an increase of a factor of only 1.5 for a station -- approximately 60 mi from ground zero. On the distant edge of the local fallout pattern only a fine rain of small particles occurs and the fraction is quite insensitive to change in the mean.

For a given mean value, an increase in the standard deviation of the log-normal will cause an increase in the fraction of particles at both ends of the distribution. Since the small end of the particle spectrum does not contribute much to the fallout, the change on the small end is not noticed. The depletion of the center of the distribution shows up as a decrease in fraction at intermediate distances with increasing σ; the augmentation of the large end shows up as an increase in fractions at very close stations with increasing σ. Thus an increase in $\sigma_{\log r}$ from .27 to .37 decreases the fraction slightly in the area where the center of the distribution falls and doubles or triples the fraction in the region close to ground zero.

We believe that the distribution of activity with particle size is determined more by the conditions of the burst --the temperature obtained and the nearness to the surface --than by the nature of the underlying surface. Until further evidence to the contrary can be presented, we will assume that the distribution of activity with particle size for surface-

burst weapons will be that of a log-normal with a mean of 1.65 and a standard deviation of 0.30.

III. SPACE DISTRIBUTION OF ACTIVITY

The second parameter which must be taken up in some detail is the distribution of the radioactive particles in space at the time of stabilization of the cloud. The study of the space distribution of activity has a long history and, in the early days, some very conflicting reports. The early reports, that is, the reports of all of the tests up to the Redwing series, were based on observations of the visual cloud. For some of the smaller yields, the toroidal circulation was not apparent, and it was therefore thought that there was a jet of material blasted into the air, and that there was considerable material at all levels. However, after some of the larger shots in the Pacific, when the toroidal circulation became evident and after some of the reconstructions which were done at the Weather Bureau[5] and at RAND,[2] it was realized that the activity was largely confined to the mushroom, and that there should be a concentration in the core of the torus. There was, however, no evidence as to the ratio of activity in the mushroom or top part of the cloud to that which was in the stem.

Based on a reconstruction from the fallout pattern, Ref. 2 indicated 90 per cent in the mushroom and 10 per cent in the stem. The dimensions of the cloud, which were used in all of the early reports, are those observed, although it was recognized that water vapor played a great role in defining the limits of the visible cloud, particularly near the stabilization time. Kellogg[10] has reported in great detail on the early studies of dimensions of the cloud as well as the means for measuring and correcting for such things as atmospheric winds and optical problems.

One of the problems which arose with the Castle-Bravo test was the

tremendous horizontal expansion of the cloud just at stabilization. It was pointed out in Ref. 11 that if the radioactivity was indeed spread as far as the visible cloud and if constant concentration with radius was assumed, it would be difficult to explain the high concentration of fallout that was observed from the Castle-Bravo shot. Therefore, the idea of an effective radiological diameter which was somewhat smaller than the final visible diameter was introduced.

The observations of the toroid and studies of smoke rings suggested that most of the debris should be concentrated in a doughnut-shaped space in the cloud. It was not until rockets measuring radioactivity were shot through the clouds during several of the Redwing tests, however, that this hypothesis was adequately confirmed.(7) These shots also indicated that the amount of radioactivity in the outer reaches of the visible cloud was indeed extremely small, and that the effective radiological diameter was much smaller than that of the visible cloud.

The radiological measurements which were made from Redwing rockets simply reported the flux of gamma rays or the roentgen dose encountered by rockets as they flew along trajectories through the clouds. In "Fallout Studies During Operation Redwing,"(7) the first reports of the results of these rocket measurements were given. The only set of measurements which were of particular interest in this project were those of the Zuni cloud. Other clouds were measured but they were formed by airburst or barge shots; also, in some cases, too few rockets penetrated the cloud to make the analysis usable.

The basic rocket data was greatly smoothed and idealized to obtain the desired distribution from the Zuni data. These smoothed values were numerically integrated over the volume swept out by the figures of revolution

formed by rotating the contour lines about the axis. Each grid value was then divided by the integrated value to yield the fraction of the device per cubic kft at each of the grid intersections. These values were then integrated at each height over the area of the circle defining the cloud at that level in order to arrive at the distribution of activity as a function of height. Figure 4 shows this distribution in fraction per kft. The distribution shown in Fig. 4 is a very much idealized representation of the fraction of device per kft for the Zuni shot of Operation Redwing.

In order to determine the radial distribution, the values of concentration were integrated over height for various values of radius. The resulting distribution of activity per kft^2 as a function of radius is shown in Fig. 5. Again, this is an idealized representation of the Zuni shot, but it does show the reality of the concentration in the toroid. The peak concentration close to the center and the small values at great distances demonstrates why the combination of the visible cloud radius with a constant radial distribution failed to produce sufficiently intense radiation on the Castle-Bravo shot.

Before going on with the problem of scaling these results to different yields, it is necessary to discuss the sensitivity of the fallout pattern to variations of these particular distributions. The radial distribution will be considered first because it has little effect on the pattern. Consider a single layer of particles of varying sizes. As the particles fall to the ground at different rates, the overlapping of the rings will tend to obscure the low concentrations in the middle of the initial distribution. In order to demonstrate this effect in an actual pattern, the computing model was used to compute, with a very simple wind structure, a

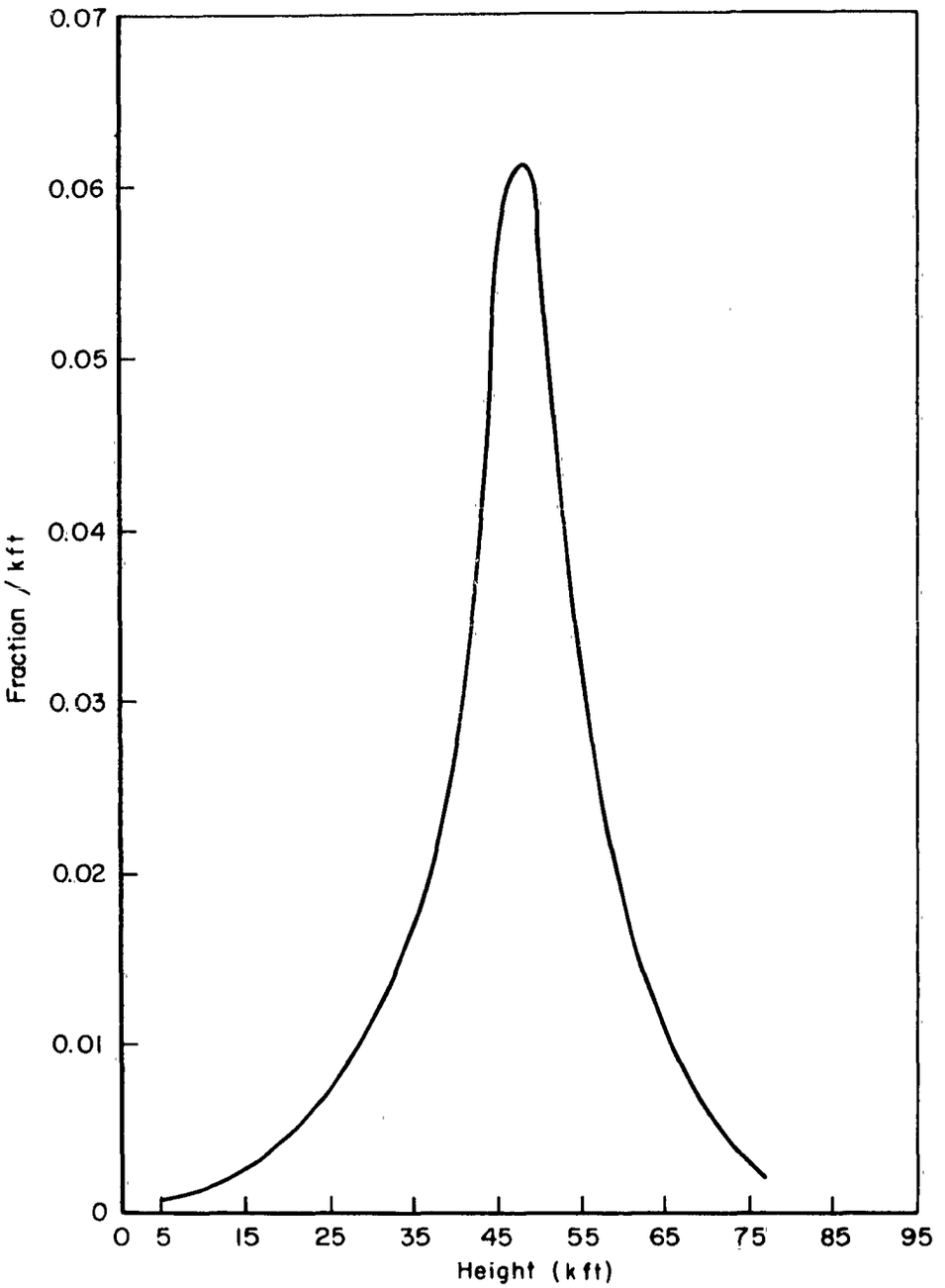

Fig. 4 — Smoothed distribution of activity with height from Zuni rocket data

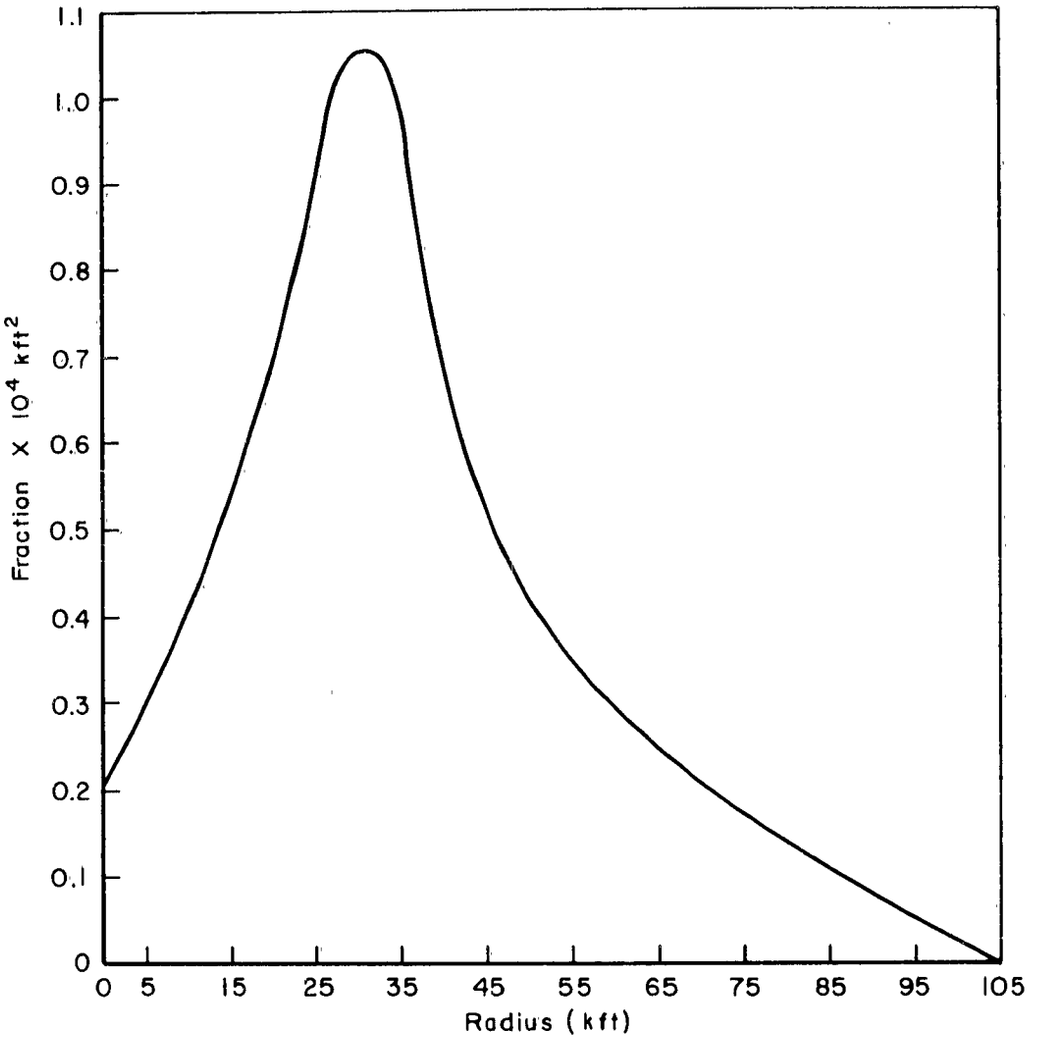

Fig. 5 — Smoothed distribution of activity with radial distance from cloud center from Zuni rocket data

pair of patterns, one based on the distribution shown in Fig. 5 and the other on a constant concentration to an effective radiological radius.

Figure 6 shows a comparison of the cross section of the resultant fallout pattern for two radial distributions at a point downwind which is representative of all downwind cross-sections. It can be seen that the correct radial distribution yields a more peaked cross-section with a slightly wider base, indicating a spread of small fractions over a wider area. As will be seen later, the edges of the pattern cannot be precisely determined in any event, so that the use of an effective radiological radius with a constant concentration is a good method of approximating the radial distribution.

The effect of changes in the elevation of the activity peak shown in Fig. 4 was also checked by machine computations. It would have been desirable to check the entire course of the distribution but there were not enough ground measurements to provide a reasonable test. In order to test the effect of changes in height of the distribution, the shape of the distribution curve was preserved. Calculations were made for the fraction down for the Zuni shot from the distribution as shown in Fig. 4, and also from a distribution with the height of the peak concentration raised by 5000 ft. The variation of fallout at the close-in stations was practically unchanged, but at YAG-40, further out, there was a marked increase. This is due to the fact that material from the peak of the activity-height distribution was made to reach YAG-40 when the peak height was raised. Since the original height distribution fit YAG-40 very well over a rather large range of activity-size distribution, it may be concluded that the activity distribution, derived from the rockets as shown in Fig. 4, was about correct.

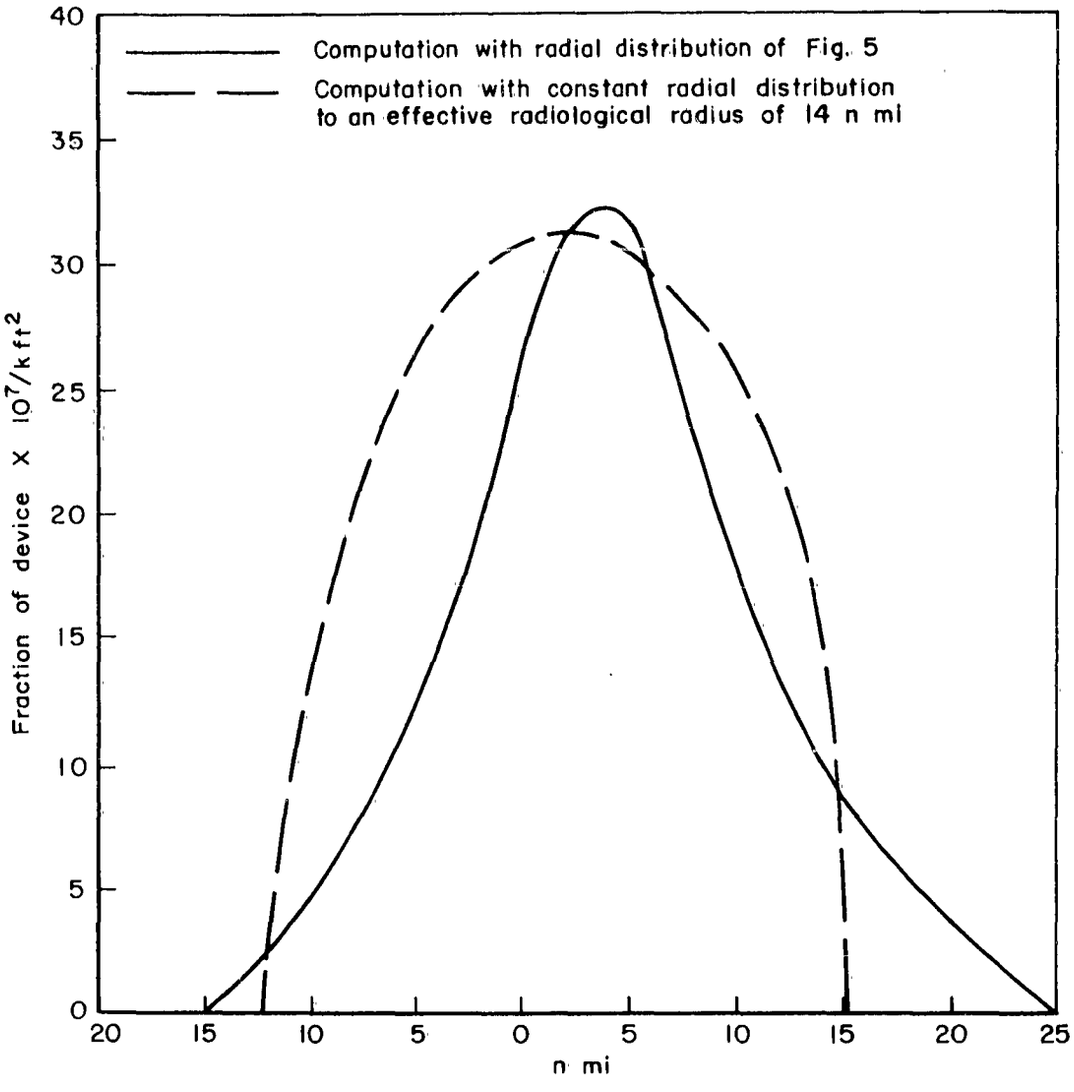

Fig. 6 — Cross section, 80 miles downwind of ground zero, for two radial distributions

Washington D.C. mean winter winds

Having determined distributions of activity with height from the Zuni shot, it is necessary to provide some method for scaling these distributions to other yields. For such a scaling, recourse must be made to visual observations because the radiological measurements are insufficient. The variation of the center of a cloud in the tropics, as deduced by Kellogg,[10] is shown in Fig. 7 together with the height of the top and bottom of the Redwing clouds as reported at seven minutes in Cloud Photography.[12] The agreement between Kellogg's analysis and the observations is extremely good. Rough estimates of the height of the maximum of activity for Zuni, Cherokee, and Navajo shots are shown by the large circles in Fig. 7. The best scaling that can be deduced from this meagre data is that the peak height of activity is coincident with the base of the visible cloud. The line of best fit to the base of the visible cloud can be expressed as

$$H(\text{kft}) = 42\ Y^{0.115}\ (\text{MT})$$

for yields greater than 300 KT in tropical atmospheres. For other atmospheric conditions, it is recommended that Kellogg's curves be used with a correction to the base of the visible cloud.

In order to scale the radial distribution, the concept of effective radiological radius with a constant concentration will be used. An effective radiological radius of 85 kft with a concentration of 4.4×10^{-5} parts per kft^2 was chosen as a fair representation of the Zuni distribution shown in Fig. 5. A plot of cloud radius at the time of stabilization and at end of growth (see Fig. 8) was taken from Ref. 10. To this plot was added the seven-minute visual radius, as taken from Ref. 12. The single point of the Zuni effective radiological radius was plotted also. The

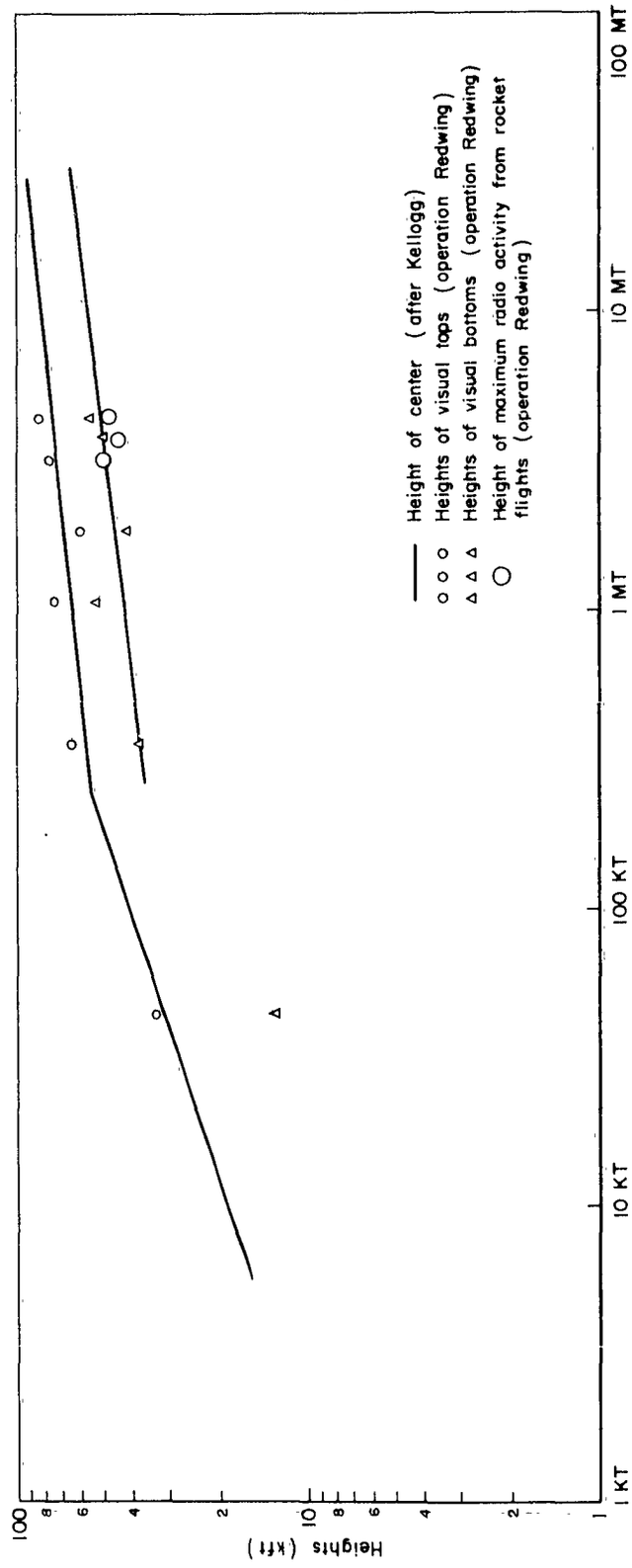

Fig. 7 — Height of top and bottom of visible atomic clouds at seven minutes after detonation

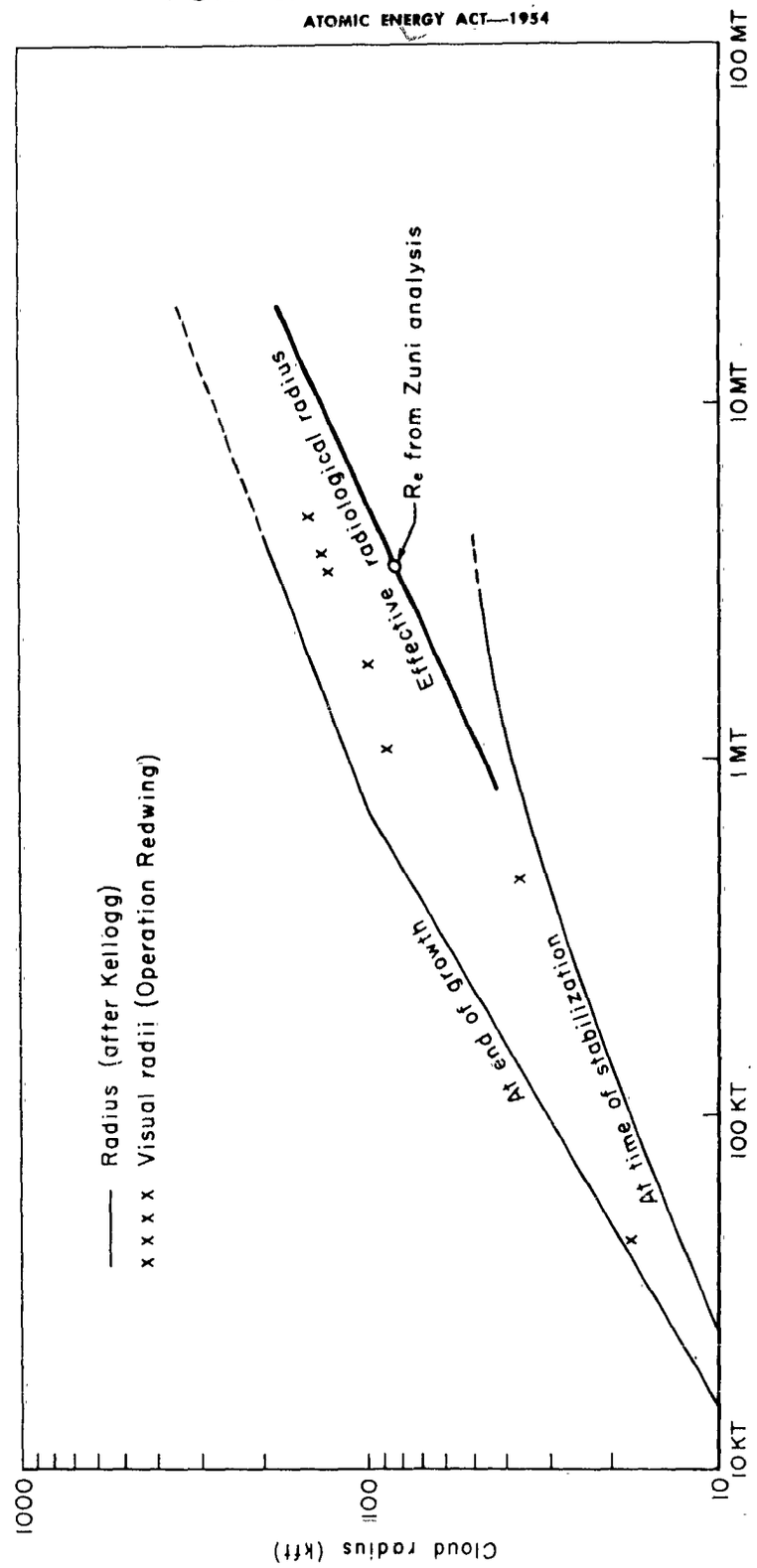

Fig. 8—Visible and effective radii of nuclear clouds

scaling of the effective radiological radius was then taken to be a line through 85 kft at 3.4 MT, which is congruent with the other curves of visible radius. This may be expressed in the range above 300 KT as

$$R_e(\text{kft}) \approx 45\ Y^{0.466}\ (\text{MT})$$

These scaling laws should be good approximations for most cases. It must be emphasized, however, that the equations are derived for tropical atmospheres. By a judicious subjective correction for atmospheric conditions following the guide lines of the Machta-Kellogg theory of the rise of the cloud, reasonable resolutions of the radiological scaling may be made.

IV. VERTICAL TRANSPORT

At the time of stabilization, the activity is distributed over a region of space and most of it is carried by small, solid particles. A study of these particles indicates that they are irregular shapes with a density of about 2.5. The density is apparently partly a function of the material of which they are composed and the nature of their formation. The value of 2.5 has been chosen as being very close to the average value of particles formed from both Nevada sand and Pacific coral.

As the circulation of the cloud dies out, gravity will impart a downward force which will rapidly be balanced by the viscous force of the air. The resultant terminal velocity of the particles will cause them to settle to the earth at a rate dependent upon their size. It is obvious that variations in density and shape will cause variations in the fall rate, but, for a first approximation, it can be assumed that the particles are spheres of density 2.5.

There are three different regimes which govern the terminal velocity of the particles in still air. The extremely small particles in the high atmosphere may be the same order of magnitude as the mean free paths of the molecules of air; therefore the corrections for mean free paths must be used. The particles in the range from about 15μ radius to about 25μ radius are large, compared to the mean free path, and yet have sufficiently small velocities to permit the use of Stokes' approximation. The larger particles must be treated by the aerodynamic equations involving the drag coefficient, which is a function of the Reynolds number, which, in turn, is a function of the speed of the particle and the particle size.

In the Stokes law range, the familiar equation for fall velocity is

$$W_s = \frac{2}{9} \frac{r^2 \rho g}{\eta}$$

where r is the particle radius, ρ is the particle density, g is the acceleration of gravity, and η is the coefficient of viscosity of the air. For the small particles this must be modified by the effect of the mean free paths. The correction factor for mean free paths, according to Kennard,[13] is

$$M = 1 + \frac{L}{r}\left(1.23 + 0.41 \exp \frac{0.88\ r}{L}\right)$$

where M is the factor which must be multiplied by W_s to obtain the true terminal velocity and L is the mean free path of the air molecules. For the larger particles the viscous force on the particles is given by

$$F_D = \frac{1}{2} \rho_a \pi W_r^2 r^2 C_D$$

where F_D is the viscous force on the particles, W_r is the large particle velocity, ρ_a is the air density and C_D is the drag coefficient. The relation of the drag coefficient to the Reynolds number for smooth spheres is shown in Fig. 9. The Reynolds number, in turn, is a function of W_r, r, ρ_a, and η

$$R_e = \frac{2 \rho_a r W_r}{\eta}$$

By equating the drag force, F_D, to the gravitational force, F_g, where

$$F_g = \frac{4}{3} \pi r^3 \rho g$$

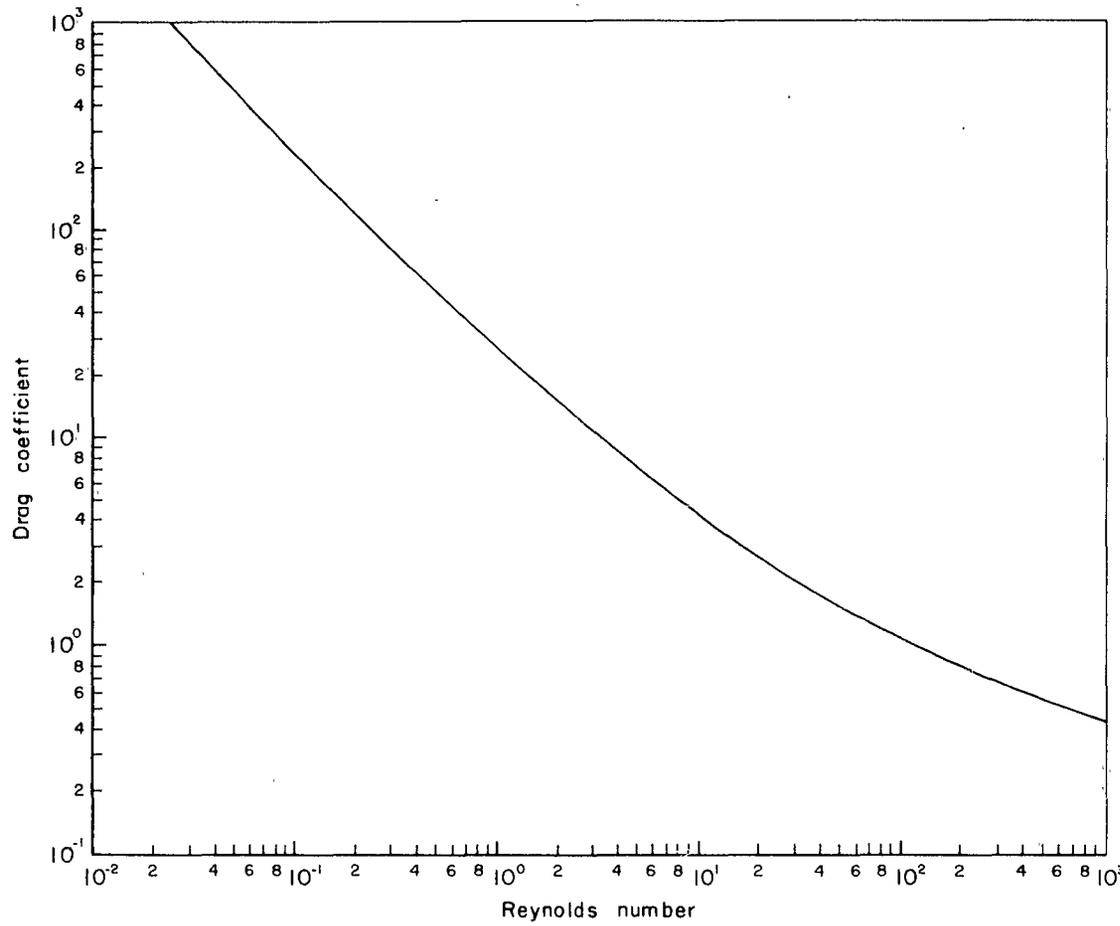

Fig. 9 — Drag coefficient for spheres as a function of Reynolds number (after Goldstein [15])

an equation involving the speed, W_r, the radius, r, the drag coefficient, and various constants is obtained. Figure 9 relates C_D to the Reynolds number and the definition of the Reynolds number relates it to the size and the speed. Because the relationship defined by Fig. 9 is not amenable to a mathematical analysis, the computations of W_r were performed by an iterative scheme outlined by Langmuir.(14) Figure 10 shows the vertical velocities of a selection of particles representing the full range of terminal velocity regimes. The New Standard Atmosphere(16) was used for the atmospheric parameters. The correction factor M, for the 0.5μ particle at 100 kft, is ~10. At the other end of the graph, the aerodynamic fall of a 600μ particle is a factor of 10 smaller than rate of fall of the Stokes law.

There is considerable uncertainty about using the drag coefficients for spheres to calculate the terminal velocities of fallout particles. In order to assess the possible error, an experiment was performed to measure the drag coefficient of simulated fallout particles as a function of the Reynolds number (Ref. 17). Calibration experiments on spheres indicated that technique was accurate to within about five per cent. The results on the fallout particle models showed only slight deviations from this sphere approximation except for four particles which were several times larger in one dimension than in the other two. Since most fallout particles do not deviate greatly from a spherical form, the drag approximation could introduce an error of less than 10 per cent, a small error, compared with some of the other uncertainties in the data.

The terminal velocities of the particles are only part of the total vertical transport. The effects of the vertical motions of the atmosphere must be included to determine the true transport relative to the earth. This

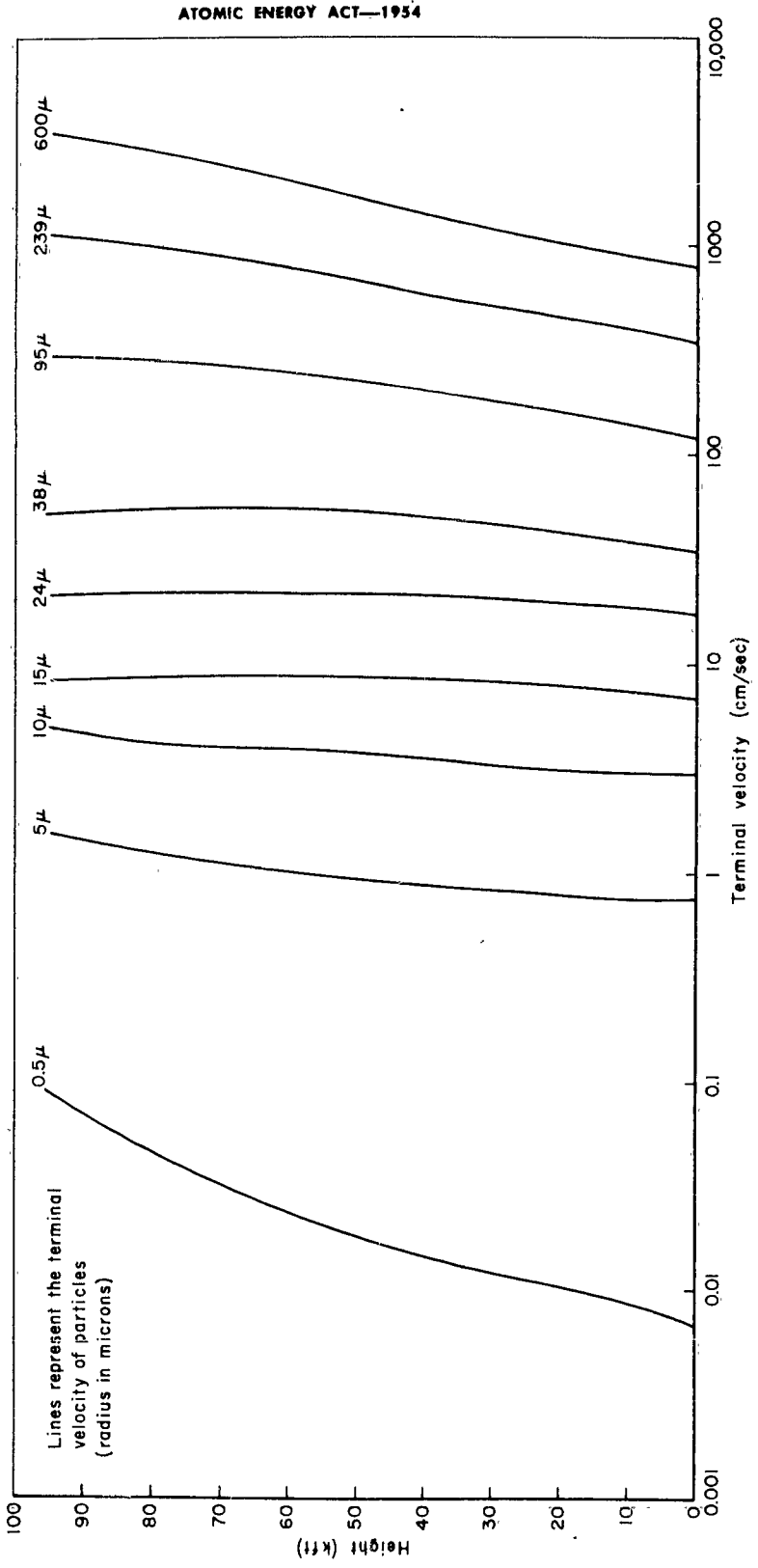

Fig. 10 — Fall velocity of spherical particles

effect is not simply an additive one because the relative motion of the air past the particles produces accelerations which are not necessarily linear.

In order to make a preliminary estimate of the effect of vertical motion of the atmosphere, the Smoluchowski equation may be used

$$\frac{\partial P}{\partial t} = K \frac{\partial^2 P}{\partial z^2} + c \frac{\partial P}{\partial z}$$

where P is the probability that a particle originating at a height z_o will arrive at a height z at some time t. K is the coefficient of diffusion and c is the terminal velocity of the particle. The assumptions which lead to this equation are that the air motions affecting the particles are completely random, and that the force of attraction is constant.

As can be seen, this is merely an extension of the diffusion equation to account for the gravitational attraction. This equation can be solved with the boundary conditions: (1) that the particle is at height $z = z_o$ with probability 1 at $t = 0$; and (2) that the particles stick to the ground when they reach $z = 0$. The equation for the probability that a particle will reach the ground between t and t + dt is then

$$P(0,t) = (4\pi t K)^{-1/2} (z_o/t) \exp - \left[\frac{z_o^2}{4Dt} - \frac{Cz_o}{2D} + \frac{C^2 t}{4D} \right]$$

This equation was numerically integrated for $z_o = 17$ km, $K = 1000$ m^2/min and 4000 m^2/min for values of C = 2 m/min and 12.5 m/min. The resulting curves are shown in Fig. 11. The velocity values correspond roughly to a 10μ particle and a 25μ particle respectively.

Figure 11 should not be considered as a quantitative estimate of the probability of the particle reaching the ground in a given time, but it does

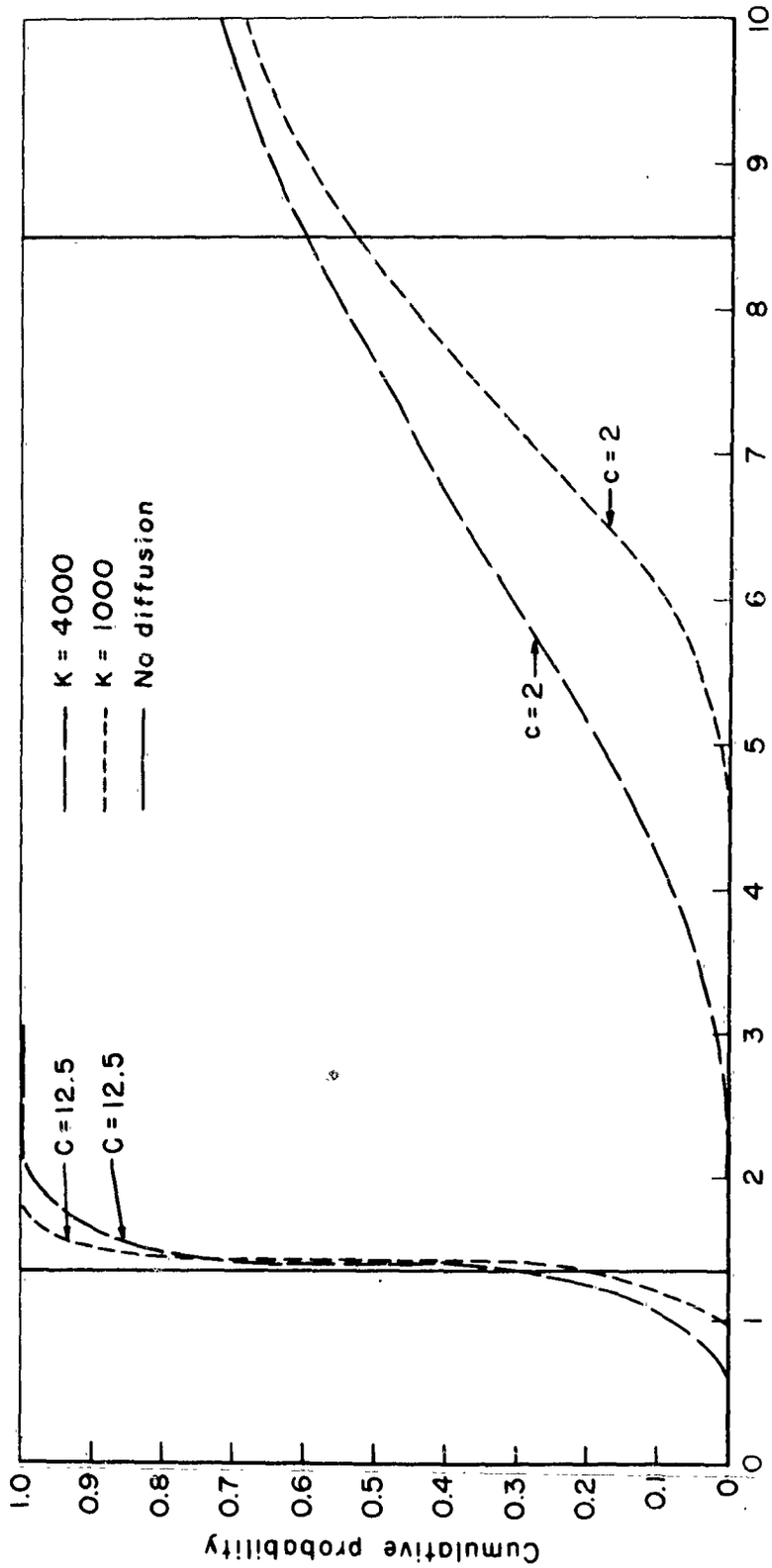

Fig. 11 — Probability of particles reaching the ground as a function of time

provide a qualitative estimate of the variation in position which must be expected due to the vertical component of turbulent fluctuations. Thus, the computation of the position of a 10μ particle which neglects the vertical turbulence is almost certain to be wrong. On the other hand, the probability is large that the 25μ particle will land within a few hours of the computed time. For larger particles, of course, the spread will be even less.

For very large-scale vertical motions of the atmosphere it would be entirely proper to add the vertical velocity to the terminal velocity in order to determine the vertical transport. This procedure, however, would be of little practical use, because large-scale motions have small magnitudes relative to the terminal velocity of large particles, and small magnitude with respect to the small-scale uncertainties for the small particles. These vertical transport effects define a limit to the utility of the direct computation of fallout. For particles which take more than about 12 hours to fall through still air, the error caused by vertical turbulence is large enough to completely invalidate the computing process. It may be possible to develop procedures for statistically including turbulent effects on the particles to arrive at expected or most probable values of deposition, but the crude approach presented here is not sufficiently precise to attempt such procedures at this time.

V. HORIZONTAL TRANSPORT

As the particles fall from their positions in the stabilized cloud, they are transported horizontally by the wind. The force that the horizontal components of the wind exert on the particles is the same sort of viscous or aerodynamic force as that discussed in the previous section. In the absence of a driving force, however, the relative velocity is rapidly reduced to zero and the particles travel essentially with the wind. This cannot be precisely correct, because changes in the horizontal wind speed will require accelerations of the particles. The lag time of even the largest particles, however, is apparently small compared with the rate at which the particles experience velocity changes; therefore it may safely be assumed that the horizontal wind velocity is equal to the horizontal particle velocity.

If $V(x,y,h,t)$ is the horizontal air velocity following the particle, then the horizontal displacement, D, is given by

$$D = \int_0^T V(x,y,h,t)\, dt$$

If it is assumed that the vertical velocity is determined by the terminal velocity, the

$$W(r,h) = \frac{dh}{dt}$$

and the transport equation may be written as

$$D(r,h) = \int_0^H V(x,y,h,t)\, \frac{dh}{W(r,h)}$$

where it has been indicated that D is a function of the particle size and

the initial height of the particle. The assumptions regarding the vertical velocity W have already been discussed.

The problem posed by the nature of the horizontal wind must be considered. In most of the early work, the wind was considered as variable only in the vertical. The effect of time and space variations were included in some of the reconstructions of initial cloud parameters by the Weather Bureau.[5] The model presented in A New Model For Fallout Calculations[18] provides for an interpolation, in time and space, from observed winds, to estimate the wind on the particle at a rather close grid of points in time and space. Any deviations of the actual wind on the particle from the interpolated wind will cause errors in the computed position.

An approximate analysis of the errors in displacement were made to indicate the magnitude of this error. The details of the analysis are presented in Ref. 18. Table 1 shows the ratio of the circular standard error of the displacement vector, σ_D, to the assumed circular standard error of the deviations of the actual wind from the interpolated wind, σ_ϵ, for a few particles. This table shows, as did Fig. 11, in Sec. IV, that the smaller particles are so subject to small-scale errors that precise location is impossible.

Table 1

RATIO OF σ_D/σ_ϵ AS A FUNCTION OF INITIAL HEIGHT AND PARTICLE RADIUS

Height (kft)	Radius (μ)			
	24	60	151	600
10	3.101	.747	.243	.063
20	4.160	1.023	.326	.084
30	5.000	1.196	.375	.095
40	5.633	1.321	.412	.105
60	6.578	1.506	.464	.114
80	7.272	1.628	.491	.118
100	7.883	1.701	.512	.118

The effect of the magnitude of the wind on a fallout pattern is an important consideration. In the case of no wind, the pattern would consist of the projection of the vortex ring upon the ground, symmetrically around ground zero. This would be a relatively small pattern of high concentration. On the other hand, a strong wind would carry small particles greater distances than the large particles and would therefore produce a more extensive pattern, but one of lesser intensity. In order to examine this effect the "single wind model," developed in Simplified Model For Fallout Calculations[19] and briefly outlined in Sec. VI, was employed. The results are shown in Figs. 12-14. Figure 12 shows how the value of the maximum fraction of the debris (roughly the same as the maximum "hot spot") decreases with increasing wind velocity. Figure 13 shows the distance from ground zero at which this maximum fraction is found. The dashed portion of the line on Fig. 13 indicates that the maximum over this range of winds is not a definite point but rather a plateau of high concentration. Figure 14 shows the fraction of debris as a function of distance from ground zero along the line of maximum concentration for three values of the mean wind velocity. This figure indicates that, as the wind velocity is increased, the material is spread in such a way that the maximum decreases and the small fractions are extended to greater distances. As indices of the general nature of the wind effects, the generalizations shown in these three figures are useful. They should not, however, be accepted as representations of real fallout patterns.

If fallout patterns are to be forecast, it is necessary to forecast the wind values to be used in the transport equation. It is well known that wind forecasting is an uncertain art. In order to try to extrapolate the degree

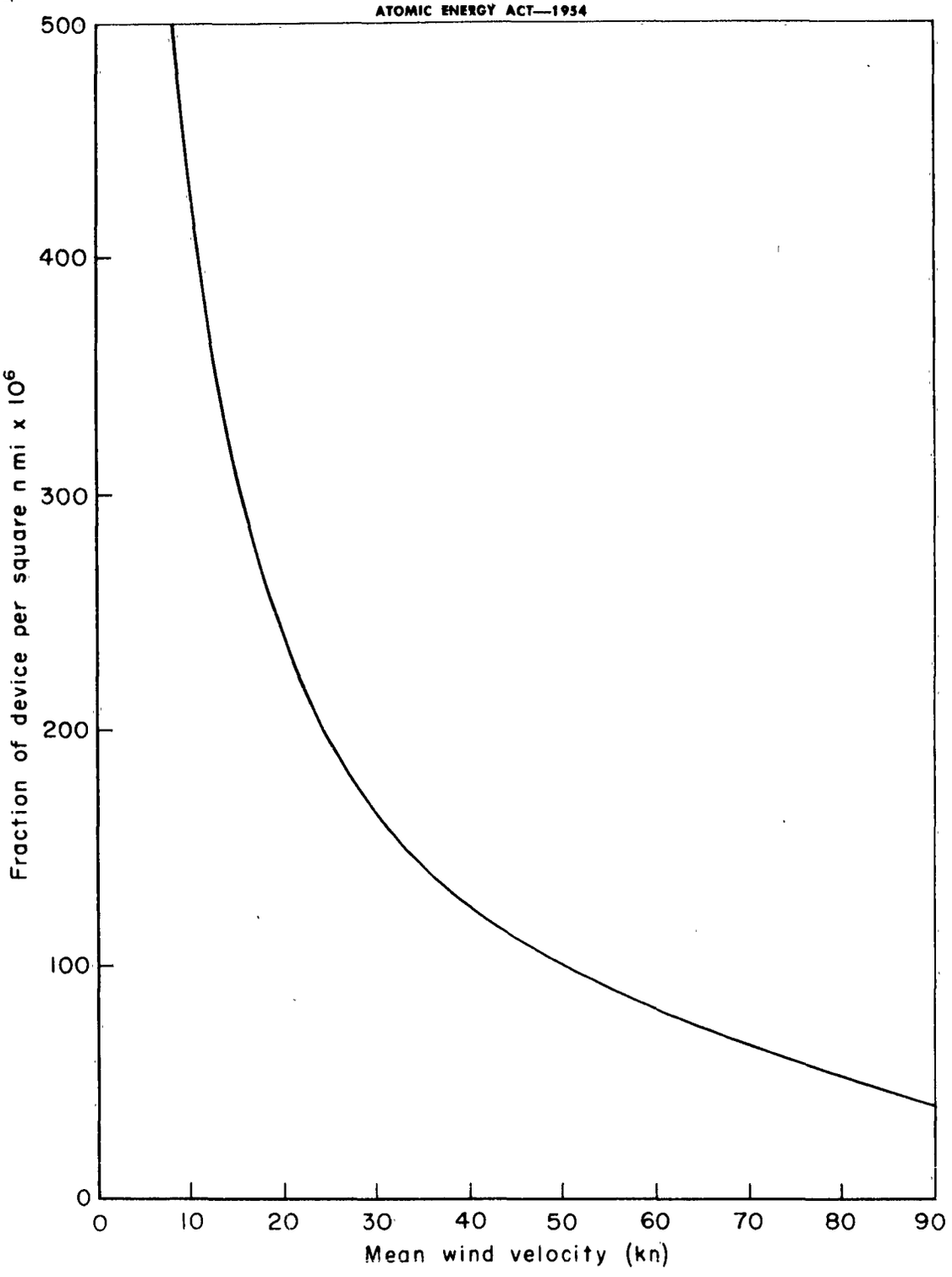

Fig. 12 — Maximum fraction of device as a function of mean wind speed

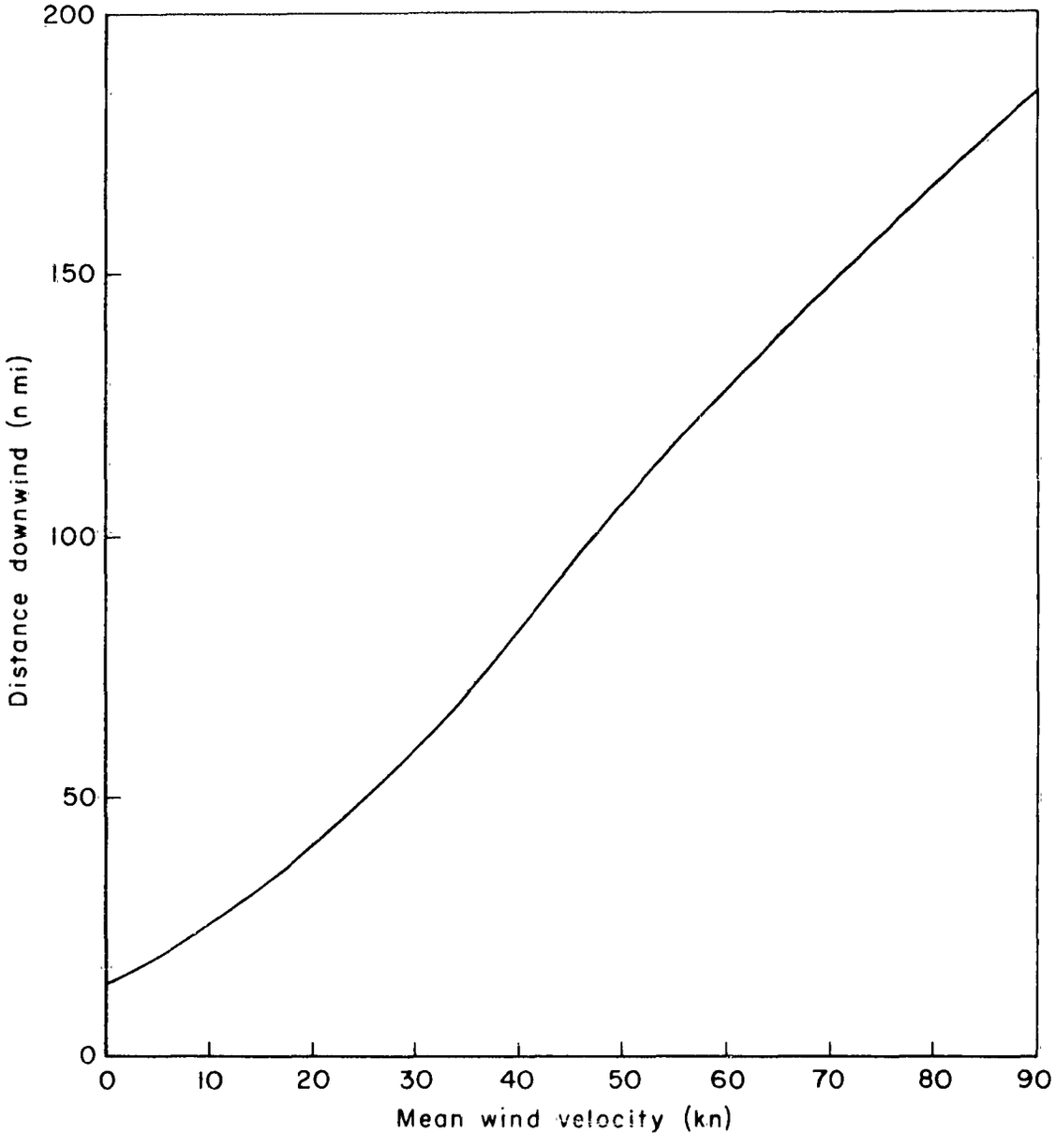

Fig. 13—Distance of maximum fraction from ground zero

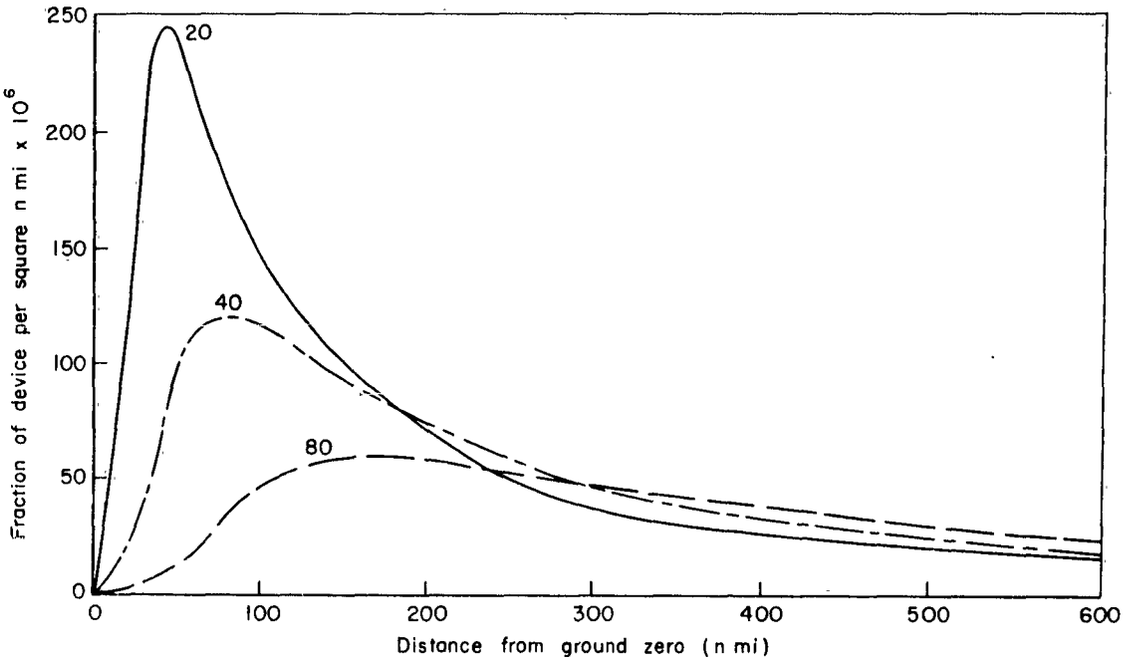

Fig. 14 — Fraction of device along axis for $\overline{V}$ = 20, 40, and 80 knots

of success which might be realized in this art in the next few years, a study of the application of numerical forecast techniques for the fallout problem has been attempted at RAND. This study, Graphical Methods For The Quantitative Prediction of Close-In Fallout,(20) indicates that useful numerical forecasts can be made in some instances. The chief difficulty, which is peculiar to fallout problems, is the scale of motion which must be considered. One of the chief conclusions in Ref. 20 is that much more detailed observation and computation is required to provide the necessary forecast precision. A concomittant of the small scale which must be considered is the removal of the geostrophic assumption from the basic prediction equations. A suitable alternative assumption was proposed and tested with remarkable success.(20)

The forecast scheme used in Ref. 20 is not intended to be a routine method for fallout forecasting. It shows, however, that the problem of forecasting winds for the prediction of fallout may be soluble by the proper application of modern forecast methods. For extremely good forecast of the fallout patterns, the numerical approach offers the best and most reliable method for making such predictions.

VI. SYNTHESIS OF FALLOUT PATTERN

The previous four sections have taken up, in some detail, the four major facets or inputs of the fallout computation model. This section describes the methods used to combine these basic components into a computation of the fraction of the radioactivity at a set of points on the ground.

It has already been assumed that the distribution of activity with height, particle size, and cloud radius are independent of one another. Let the activity function be defined so that the integral of the product of the distribution functions over the entire volume of the cloud and over all particle sizes is equal to one. Then, if this function is integrated over only those particle sizes and initial heights which land at a particular point, the result will be the fraction per unit area at that point. The transport equation can be used to define the limits of particle size and height at the point, and in this manner the problem can be solved.

Unfortunately none of the functions are immediately amenable to a simple mathematical solution. In order to carry out the indicated integration, two simplifying procedures have been developed: (1) The integration can be done numerically by defining the functions empirically, and (2) The functions can be approximated by tractable equations and a mathematical integration can be made. Both of these techniques have been used; the first is reported in Ref. 18 and the second in Refs. 19 and 21. The method of Ref. 18 will be briefly reviewed and cast into graphical terms in order to demonstrate the procedure.

The first step is to compute the displacement for a series of particle sizes, each from a number of different heights, and to make a plot of the ground positions of these particles as in Fig. 15. Then some point where it

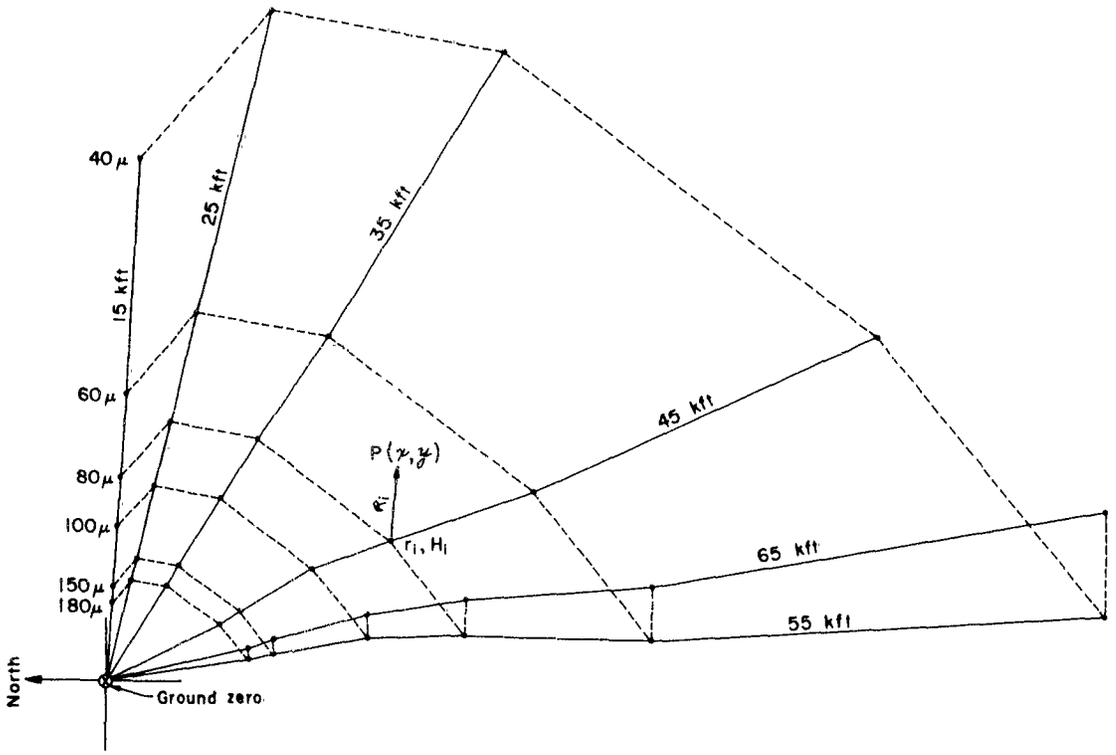

Fig. 15 — Plot of the positions of several particle sizes on the midline of the cloud from several heights

is desired to compute the fraction of the device is chosen; call this point $P(\chi,\gamma)$. Consider now a particle from height H_1, of size r_1, which was initially in the center of the cloud. This will land at a distance R_1 from the selected point P. Therefore, with the assumption of no relative diffusion of particles, a particle of size r_1, from height H_1 which was initially at a distance R_1 from the center of the cloud will land at the point $P(\chi,\gamma)$. The activity density contained on particles of size r_1, from height H_1 at a distance R_1 from the center of the cloud is given by the product of the three activity density distributions. If the activity density functions for all particles, r_i, from all heights, H_j, and radii, R_k, which land at the point, $P(\chi,\gamma)$, are determined, they can be integrated numerically over particle size and height. The resulting number is a density, or fraction of device per unit area, at the point on the ground.

This integration forms the basis of the computing procedure presented in Ref. 18. The computational procedure has been used to test the distributions against the observations of Operations Castle and Redwing with considerable success to distances up to about 100 mi downwind.

The machine computation is ideally suited to testing the variation of parameters for comparison with observations because of the detailed manner in which the winds are treated. In order to investigate the changes of the pattern with wind, however, it is more convenient to simplify the problem so as to permit mathematical integration which will bring the main effects of wind velocity into clear focus. The simplifications invoked were the use of an effective radiological radius for the cloud, the assumption of a constant concentration with height over a layer, and the approximation of the log-normal activity-particle size distribution with an exponential function

for particle sizes greater than 25μ. By applying the mean value theorem to the transport equation, the entire wind structure is replaced by a mean wind. The variation of some salient features of the fallout pattern with the mean wind could thereby be computed with less time and effort than that required by the complex machine operation. The details of the computation are reported in Ref. 19. Figure 16 is a graphical representation of the mathematical integration. It shows the fraction of the device per unit area as a function of wind velocity and distance from ground zero along the axis.

In order to provide a simplified method of computation which will permit more detail than a single integrated wind, the basic single wind model was modified to use integrated winds to a series of heights. This is accomplished by treating different layers of the cloud as separate entities. The basic equations were solved for six 10-kft layers and the results of each calculation were presented in graphical form. Scaling laws were developed to permit the graphs to be used over a range of yields for approximately one to 20 MT. By making a plot of the down position of a few particles (see Fig. 15) and applying the single wind method to each layer separately, it is possible to compute the fraction of the device at a point by summing the results of each layer. Reference 21 presents the details of this analysis. Figure 17 shows the results of applying this layer method to the Zuni shot of Operation Redwing. The results may be considered as an excellent approximation to the estimates made from observations, particularly when one compares Fig. 17 with Fig. 3.

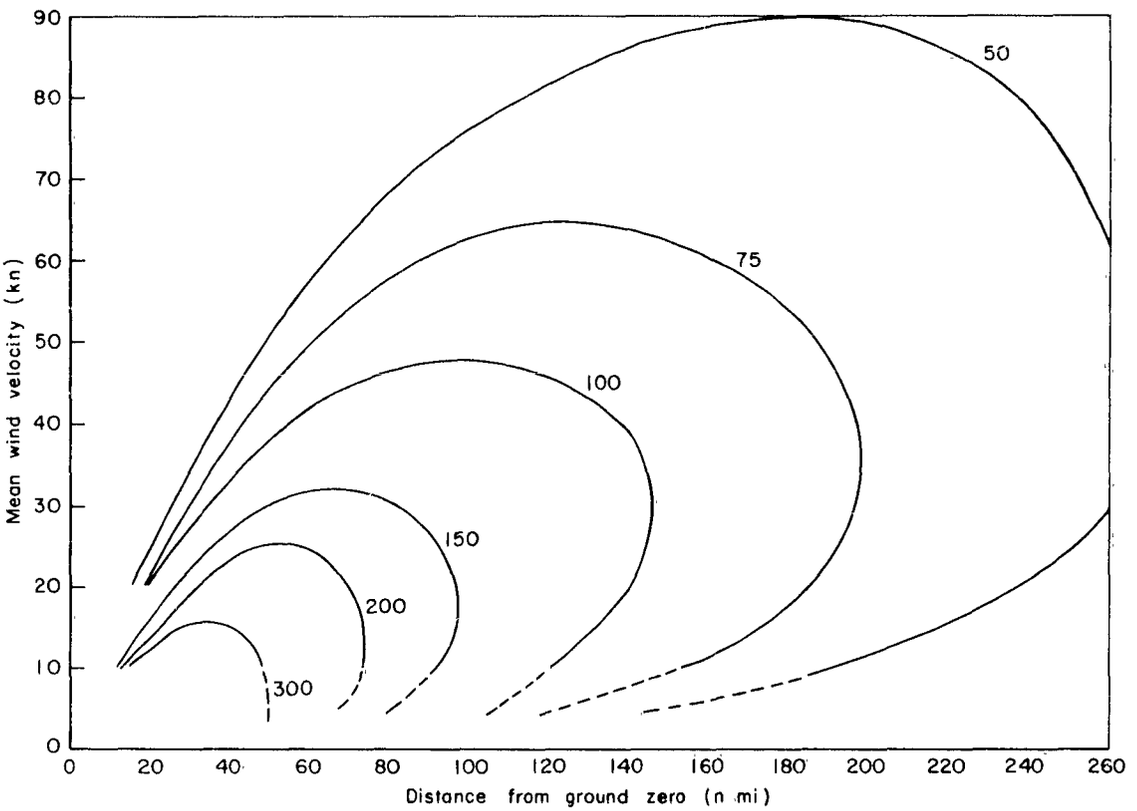

Fig. 16 — Fraction of a 3.5 MT devices x 10^6 per n mi^2 along the axis of the pattern as computed from the single wind model

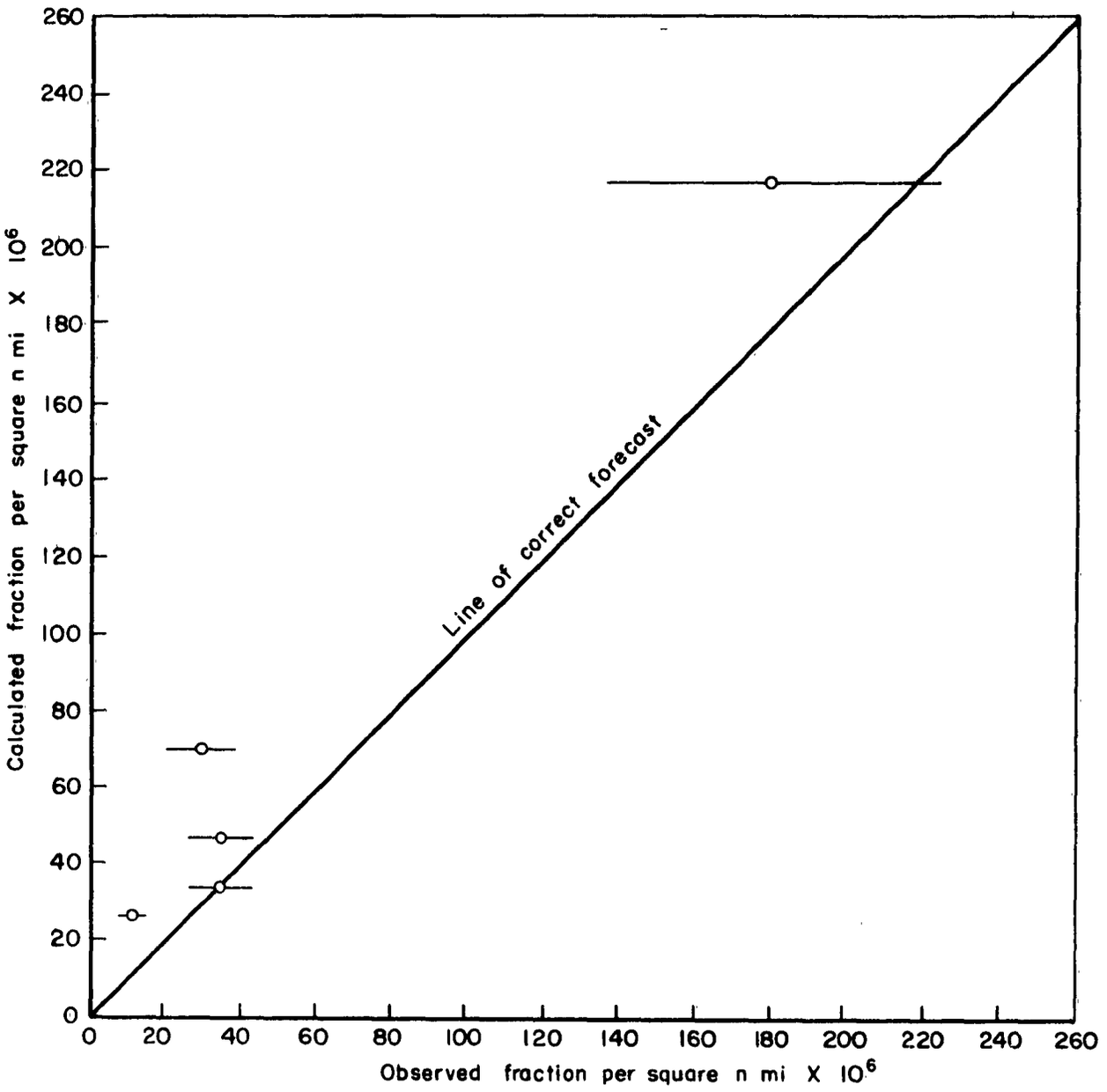

Fig. 17 — Calculated vs observed fallout for the Zuni shot of operation Redwing. Calculations made by the six — layer, hand-computing model

VII. CONCLUSION

The foregoing brief summary of RAND's studies in the field of radioactive fallout should point up several salient facts. Perhaps the most important of these facts is the absence of accurate measurements of the basic parameters necessary to predict or compute fallout patterns. The direct measurements made to date do not provide either the distribution of activity with particle size or the distribution of activity in space. As yet there has been no attempt made to determine the average falling velocity of actual fallout particles. The restricted number of test sites has practically prohibited any study of the effect of soil type on the resulting fallout particles. And, finally, the current methods of wind measurement and forecasting are inadequate for a precise attack on the problem, even if the other factors were well known.

Despite these obvious deficiencies it has been possible to construct a useful working model for the computation of the fallout resulting from surface-burst weapons. Further, within the framework of this model, it has been possible to assess the relative effect of the various parameters on the resulting fallout patterns. The most pronounced effect is the variation in intensity caused by the wind. A change in mean wind velocity from 20 to 40 kn can reduce the value of the peak concentration by a factor of two and increase the intensity at great distances from ground zero by as much as 30 per cent (see Fig. 14).

Another parameter which has a major effect on the fallout pattern is the height of the cloud. The height of the peak of the initial space distribution is related almost linearly to the distance to which the maximum is displaced downwind from ground zero, and this varies with yield and, to some

extent, with meteorological conditions.

The distribution of activity with particle size is important, but not quite so critical as the wind and the height distribution. With the assumption that the fall rates are closely approximated by the computations for spherical particles of density 2.5, the distribution must have a shape something like a log-normal with a mode approximately at 40μ radius. Small variations from this distribution will not change the results of a computation markedly, but according to Fig. 2 it would be impossible to produce realistic results if the mode were changed by more than 10μ either way. It is necessary to note that the small-particle end of the distribution is completely undetermined. Our approach limits us to data from particles which fall in a relatively short time; thus, the small-particle end of the distribution is pure extrapolation.

The model, together with possible advances in the state of the wind forecasting art, offers some promise of a reasonably accurate prediction of fallout. The major limitations on the possibility of fallout forecasting are the lack of detailed knowledge of the initial distributions and our inability to predict the small scale motions of the atmosphere. These uncertainties should not preclude the use of forecasting as a guide to more detailed delineation of the patterns, but it is necessary to recognize the sources of error and to be aware of the uncertainties inherent in any forecast fallout pattern.

Other organizations have devoted much effort to the forecasting of fallout and have had moderate success in forecasting the patterns to be expected from the test shots. Most of the methods used are similar in principle to the methods outlined here, and the degree of success which they have attained

in operational situations points out both the usefulness of the fallout forecast and its inherent limitations.

It is our belief that the models developed at RAND during the last two years represent methods of fallout prediction which are commensurate in precision with the demonstrated ability to measure the pattern of fallout. We feel that it is possible to make improvements in the pure mechanical computing processes which will permit operationally useful fallout forecasts to be made. But we feel constrained to point out the inherent errors of this type of forecast and to warn against blind dependence on any forecast.

REFERENCES

1. The RAND Corporation, Close-In Fallout, Report R-309, September 30, 1957.

2. Greenfield, S. M., W. W. Kellogg, F. J. Krieger, and R. R. Rapp, Transport and Early Deposition of Radioactive Debris - Project Aureole (U), The RAND Corporation, Report R-265-AEC, July 1, 1954 (Secret-Restricted Data).

3. Krey, P. W., "Operation Redwing Results," Appendix B of RAND Fallout Symposium (U), S-62, April 1, 1957 (Secret-Formerly Restricted Data).

4. Henriques, F. C., "Prediction of Dose Rate and Dosage Contours as Functions of Yield and Meteorological Conditions, ORO and Technical Operations, Inc. Method (U)" Fall-out Symposium, Armed Forces Special Weapons Project 895, pp. 403-444, January, 1955 (Secret-Restricted Data).

5. Nagler, K. M., "Prediction of Dose-Rate and Dosage Contours as Functions of Yield and Meteorological Conditions, U.S. Weather Bureau Method (U)" Fall-out Symposium, Armed Forces Special Weapons Project 895, pp. 355-373, January, 1955 (Secret-Restricted Data).

6. Joint Task Force Seven, Meteorological Report on Operation REDWING, Joint Task Force Seven Meteorological Center, March 1957.

7. Van Lindt, V. A. J., L. E. Killion, J. A. Chiment, and D. C. Campbell, Fallout Studies During Operation Redwing, ITR-1354, October, 1956 (Secret-Restricted Data).

8. Rapp, R. R., The Second RAND Fallout Model: A Computational Test (U), The RAND Corporation, Research Memorandum RM-2148, April 8, 1958 (Secret-Restricted Data).

9. Triffet, T., et al., "Characterization of Fallout," ITR-1317, Operation Redwing Preliminary Report, February 1957.

10. Kellogg, W. W., Atomic Cloud Height As a Function of Yield and Meteorology, The RAND Corporation, Paper P-881-AEC, June 14, 1956.

11. Greenfield, S. M., and R. R. Rapp, Fallout Computations and CASTLE-BRAVO: A Case Study (U), The RAND Corporation, Research Memorandum RM-1855, January 16, 1957 (Secret-Restricted Data).

12. Fussel, L., and Staff of Edgerton Germeshausen and Grier, Cloud Photography, ITR-1343, May 1957.

13. Kennard, E. H., Kinetic Theory of Gases - 1st Ed., New York, McGraw-Hill, 1938.

14. Langmuir, I., "The Production of Rain by a Chain Reaction in Cumulus Clouds of Temperatures Above Freezing," Jour. Met., Vol. V, No. 5, pp. 175-192, 1948.

15. Goldstein, Modern Developments in Fluid Mechanics, Vol. I, Oxford, Clarendon Press, 1938.

16. Minzner, R. A., and Ripley, W. S., Air Force Surveys in Geophysics, No. 86, "The ARDC Model Atmosphere," December 1956.

17. Rapp, R. R., and J. D. Sartor, Rate of Fall Through the Atmosphere of Irregularly Shaped Particles, The RAND Corporation, Research Memorandum RM-2006 (ASTIA No. AD150665), November 1, 1957.

18. Rapp, R. R., A New Model for Fallout Calculations (U), The RAND Corporation, Research Memorandum RM-2115, February 13, 1958 (Secret-Restricted Data).

19. Rapp, R. R., A Simplified Model for Fallout Computations: Part I (U), The RAND Corporation, Research Memorandum RM-2193, June 9, 1958 (Confidential-formerly Restricted Data).

20. Knox, J. B., Graphical Methods for the Quantitative Prediction of Close-In Fallout, The RAND Corporation, Research Memorandum RM-2108, January 31, 1958.

21. Rapp, R. R., and P. A. Walters, A Simplified Model for Fallout Computations, Part II (U), The RAND Corporation, Research Memorandum RM-2296, November 22, 1958 (Confidential-formerly Restricted Data).

Addressee	Copies
Deputy Chief of Staff for Military Operations Department of the Army Washington 25, D.C. Att: Director of Air Defense and Special Weapons	1
Chief of Research and Development Department of the Army Washington 25, D.C. Att: Atomics Division	1
Department of the Army Office, Assistant Chief of Staff for Intelligence Washington 25, D. C. Att: Intelligence Document Branch	1
Office, Chief Chemical Officer Department of the Army Building T-7 Washington 25, D. C.	2
Chief of Engineers Department of the Army Washington 25, D.C.	
Att: ENGNB	1
Att: ENGTB	1
Office, Chief of Ordnance Department of the Army Washington 25, D. C. Att: R and D Division, ORDTU	1
Office of the Chief Signal Officer Department of the Army Washington 25, D. C. Att: Chief, Research and Development Division	1
The Surgeon General Department of the Army Washington 25, D.C. Att: MEDNE	1
U.S. Army Command and General Staff College Fort Leavenworth, Kansas Att: Archives	1

Addressee	Copies
U.S. Army Air Defense School Fort Bliss, Texas Att: Dept. of Tactics and Combined Arms	1
U. S. Army Artillery and Missile School Fort Sill, Oklahoma Att: Combat Development Department	1
Director of Special Weapons Developments U.S. Continental Army Command Fort Bliss, Texas Att: Capt. Chester I. Peterson	1
President, U.S. Army Artillery Board Fort Sill, Oklahoma	1
President, U.S. Army Infantry Board Fort Benning, Georgia	1
President, U.S Army Air Defense Board Fort Bliss, Texas	1
President, U.S. Army Aviation Board Fort Rucker, Alabama Att: ATBG-DG	1
U.S. Continental Army Command Fort Monroe, Virginia Att: ATDEV-5	3
The Infantry School Fort Benning, Georgia	1
Commandant, The Quartermaster School Fort Lee, Virginia	1
Commandant, U.S. Army Ordnance School Aberdeen Proving Ground, Maryland	1
Command, U.S. Army Ordnance & Guided Missile School Redstone Arsenal, Alabama	1
Commandant, Chemical Corps School Chemical Corps Training Cmd. Fort McClellan, Alabama	1

Addressee	Copies
Commandant, U.S. Army Signal School Fort Monmouth, New Jersey	1
Transportation Corps Library U.S. Army Transportation School Fort Eustis, Virginia	1
Commanding General The Engineer Center Fort Belvoir, Virginia Att: Asst Cmdt Engineer School	1
Commanding General Army Medical Service School Brooke Army Medical Center Fort Sam Houston, Texas	1
Commanding Officer 9th Hospital Center APO 180 New York,,New York Att: U.S. Army Nuclear Med Research Detachment, Europe	1
Director, Armed Forces Institute of Pathology Walter Reed Medical Center 625 16th Street, N.W. Washington 25, D. C.	1
Commanding Officer Army Medical Research Lab Fort Knox, Kentucky	1
Commandant Walter Reed Army Institute of Research Walter Reed Army Med Center Washington 25, D. C.	1
Commanding General Quartermaster Research and Engineering Command Quartermaster Research and Engineering Center Natick, Massachusetts Att: Technical Library	1

Addressee	Copies
Commanding General Quartermaster Research and Engineering Center Natick, Massachusetts	1
Commanding General Chemical Corps Research and Development Command Washington 26, D.C.	1
Commanding Officer U.S. Army Chemical Warfare Laboratories Technical Library, Building 330 Army Chemical Center, Maryland Att: Librarian	2
Commanding General U. S. Army Engineer Research and Development Laboratories Fort Belvoir, Virginia Att: Technical Documents Center	1
Director, Waterways Experiment Station P. O. Box 631 Vicksburg, Mississippi Att: Library	1
Commanding Officer Picatinny Arsenal Dover, New Jersey Att: ORDBB-TT	1
Commanding Officer Diamond Ordnance Fuze Laboratories Washington 25, D.C. Att: Library	1
Commanding General Aberdeen Proving Ground, Maryland Att: Ballistic Research Laboratories	1
Commanding Officer Signal Corps Engineering Laboratories Fort Monmouth, New Jersey Att: SIGEL-CD-319.1	1
Commanding General Army Electronic Proving Ground Fort Huachuca, Arizona Att: SIGPG-DCGO	1

Addressee	Copies
Commanding General U.S. Army Combat Surveillance Agency 1124 North Highland Street Arlington Virginia	1
Commanding Officer, U.S. Army Signal R&D Lab Fort Monmouth, New Jersey Att: Tech Doc Cntr Evans Area	1
Commanding Officer U.S. Army Transportation Research and Engineering Command Fort Eustis, Virginia Att: Chief Technical Services Division	1
Commanding Officer, U.S. Army U.S. Army Transportation Combat Development Group Fort Eustis, Virginia	1
Office, Chief of Transportation Department of the Army Washington 25, D. C. Att: TCACR-TC	1
Chief of Naval Operations OP-923M1C1 Department of the Navy Washington 25, D.C.	1
Chief of Naval Operations OP-36-AE Division Department of the Navy Washington 25, D.C.	1
Director of Guided Missiles (OP074) Office of the Chief of Naval Operations Department of the Navy Washington 25, D.C.	1
Chief of Naval Operations OP03EG Department of the Navy Washington 25, D. C.	1

Addressee	Copies
Chief of Naval Research (406) Department of the Navy Washington 25, D. C.	1
Chief, Bureau of Aeronautics Department of the Navy Washington 25, D. C. Att: Deputy and Assistant Chief of Bureau	1
Chief, Bureau of Medicine & Surgery Department of the Navy Washington 25, D. C. Att: Special Weapons Def Division	1
Chief, Bureau of Ordnance Department of the Navy Washington 25, D. C. Att: RE 2 Att: S.P.	1 1
Chief, Bureau of Ships Department of the Navy Washington 25, D.C. Att: Code 635	1
Bureau of Yards and Docks Department of the Navy Washington 25, D. C. Att: Logistics Planning Division Code D-300	1
Director, U.S. Naval Research Laboratory Washington 25, D. C. Att: Code 2027	1
Commander, U. S. Naval Ordnance Laboratory White Oak, Silver Spring, Maryland Att: Librarian	1
Director, The Material Lab New York Naval Shipyard Brooklyn, New York	1
Commanding Officer and Director, U. S. Navy Electronics Laboratory (Library) San Diego 52, California	1

Addressee	Copies
Commanding Officer and Director, Code 222A U. S. Naval Radiological Defense Laboratory San Francisco 24, California	4
Officer-in-Charge, U.S. Naval Civil Engineering R&E Lab U.S. Naval Construction Bn Center Port Hueneme, California Att: Code 753	1
Commanding Officer U.S. Naval Schools Command U.S. Naval Station Treasure Island San Francisco, California	1
Superintendent U.S. Naval Postgraduate School Monterey, California Att: Librarian	1
Officer-in-Charge U.S. Naval School CEC Officers U.S. Naval Construction Bn Center Port Heuneme, California	1
Commanding Officer Nuclear Weapons Training Center Atlantic Naval Base Norfolk 11, Virginia Att: Nuclear Warfare Dept.	1
Commanding Officer and Director U.S. Naval Training Device Center Port Washington, New York Att: Librarian	1
Commanding Officer U.S. Naval Damage Control Training Center Naval Base, Philadelphia, Pa. Att: ABC Defense Course	1
Commanding Officer Air Development Squadron 5 VX-5, China Lake, California	1
Commanding Officer Naval Air Sp Wpns Facility Kirtland AFB, New Mexico	1

Addressee	Copies
Commanding Officer U.S. Naval Medical Research Institute National Naval Medical Center Bethesda, Maryland	1
Commander U.S. Naval Ordnance Test Station China Lake, California	1
Director, David Taylor Model Basin Department of the Navy Washington, D.C. Att: Aerodynamics Laboratory Library	1
Officer-in-Charge U.S. Naval Supply Research & Development Facility Naval Supply Depot Bayonne, New Jersey	1
Commandant United States Marine Corps Department of the Navy Washington 25, D. C.	1
Director, Marine Corps Landing Force Development Center Marine Corps Schools Quantico, Virginia	1
Assistant for Atomic Energy Office, DCS/Operations Hq., USAF Washington 25, D.C.	1
Director of Civil Engineering DCS/Operations Hq., USAF Washington 25, D. C.	1
Deputy Chief of Staff Operations, Hq., USAF Washington 25, D. C. Att: AFOOP	1
Director of Collection and Dissemination Office, Assistant Chief of Staff, Intelligence Hq., USAF Washington 25, D. C. Att: AFCIN-1B2	2

Addressee	Copies
Chief, Guidance and Weapons Division Directorate of Research and Development Office, DCS/Development Hq., USAF Washington 25, D.C.	1
Director of Professional Services Office of the Surgeon General Hq., USAF Washington 25, D.C. Att: Aviation Medicine Division	1
Commander in Chief Strategic Air Command Offutt Air Force Base, Nebraska	1
Commander, Tactical Air Command Langley Air Force Base, Virginia Att: Director of Communications-Electronics	1
Commander, Alaskan Air Command APO 942, Seattle, Washington Att: Operations Analysis Office	1
Commander in Chief Pacific Air Forces APO 953, San Francisco, California Att: Operations Analysis Office ACS/Operations (A-3)	1
Commander, Air Defense Command Ent Air Force Base Colorado Springs, Colorado Att: Deputy for Plans Atomic Energy Division (ADLAN-A)	1
Commander (RDG) Air Research and Development Command Andrews Air Force Base Washington 25, D. C.	1
Commander, Air Force Ballistic Missile Division Headquarters Air Research and Development Command Air Force Unit Post Office Los Angeles 45, California	1

Addressee	Copies
Commander Air Force Cambridge Research Center Laurence G. Hanscom Field Bedford, Massachusetts Att: CRRT	1
Commander Air Force Special Weapons Center Kirtland Air Force Base Albuquerque, New Mexico Att: SWOI	2
Director, Air University Library Maxwell Air Force Base, Alabama	3
Lowry Technical Training Center (TW) Lowry Air Force Base, Colorado	1
Commandant, Air Force School of Aviation Medicine Randolph AFB, Texas Att: Research Secretariat	1
Commander, 1009th Sp Wpns Squadron Hq., USAF Washington 25, D.C.	1
Commander Wright Air Development Center Wright-Patterson Air Force Base, Ohio Att: Rand Project, WCOSI	3
Director of Development Planning Office, DCS/Development Hq., USAF Washington 25, D.C. Att: RAND Project Office	2
Deputy Chief of Staff, Operations Hq., USAF Washington 25, D.C.	1
Office of Director of Defense Research and Engineering Technical Library Room 3E-1065, The Pentagon Washington 25, D.C.	1

Addressee	Copies
Director Weapons Systems Evaluation Group Department of Defense Washington 25, D. C.	1
Commandant Industrial College of the Armed Forces Fort Lesley J. McNair Washington, D.C.	1
Commandant Armed Forces Staff College Norfolk 11, Virginia	1
Chief, Defense Atomic Support Agency Washington 25, D.C. Att: Document Library Branch	15
Commander, Field Command Defense Atomic Support Agency Sandia Base Albuquerque, New Mexico	1
Special Weapons Training Group Defense Atomic Support Agency Sandia Base Albuquerque, New Mexico Att: FC Technical Library	1
Commander, Field Command Defense Atomic Support Agency Sandia Base Albuquerque, New Mexico Att: FCDV	3
Commander, JTF-7 Arlington Hall Station Arlington 12, Virginia	1
Armed Services Technical Information Agency Arlington Hall Station Arlington 12, Virginia Att: TIPCR	10
Sandia Corporation Sandia Base P. O. Box 5800 Albuquerque, New Mexico Att: Mrs. Bertha R. Allen, Librarian	1

RM-2334
2-25-59
68

Addressee	Copies
Director, University of California Los Alamos Scientific Laboratory Post Office Box 1663 Los Alamos, New Mexico	1
Chief, Classified Document Unit Division P-T Information Service Atomic Energy Commission Washington 25, D.C.	2
University of California Lawrence Radiation Laboratory Technical Information Division Post Office Box 808 Livermore, California Att: Clovis G. Craig	1
U.S. Atomic Energy Commission Technical Library Washington 25, D.C.	1
For the use of Robert L. Corsbie, DBM	
PLUS one copy for: General A. D. Starbird, DMA	1

CARDS REMOVED BY: 1 ______

2 ______

3 ______

4 ______

CONFIDENTIAL

The RAND Corporation, Santa Monica, Calif.
USAF Project RAND RM-2334

SUMMARY REPORT OF RAND WORK ON THE AFSWP FALLOUT PROJECT (U) by R. R. Rapp; Research Memorandum RM-2334, February 25, 1959, CONFIDENTIAL–FORMERLY RESTRICTED DATA. 73 pp. incl. illus.

A concluding study of an investigation dealing with the physical processes of local radioactive fallout caused by surface-burst nuclear weapons, and with the development of mathematical models that would permit the computation or prediction of surface fallout patterns. This summary discusses the basic parameters needed to construct a fallout computation model, considers the relative importance, availability, and accuracy of the inputs to the model, describes the various RAND fallout models, and evaluates fallout models generally as operationally useful prediction devices. It is concluded that reasonably accurate fallout forecasts are possible through the use of mathematical models, but that the operational consumer must recognize the sources of error and the inherent uncertainties of any predicted fallout pattern.

The classification of RM-2334 is CONFIDENTIAL–FORMERLY RESTRICTED DATA; the classification of this abstract is CONFIDENTIAL.

CONFIDENTIAL

CONFIDENTIAL

The RAND Corporation, Santa Monica, Calif.
USAF Project RAND RM-2334

SUMMARY REPORT OF RAND WORK ON THE AFSWP FALLOUT PROJECT (U) by R. R. Rapp; Research Memorandum RM-2334, February 25, 1959, CONFIDENTIAL–FORMERLY RESTRICTED DATA. 73 pp. incl. illus.

A concluding study of an investigation dealing with the physical processes of local radioactive fallout caused by surface-burst nuclear weapons, and with the development of mathematical models that would permit the computation or prediction of surface fallout patterns. This summary discusses the basic parameters needed to construct a fallout computation model, considers the relative importance, availability, and accuracy of the inputs to the model, describes the various RAND fallout models, and evaluates fallout models generally as operationally useful prediction devices. It is concluded that reasonably accurate fallout forecasts are possible through the use of mathematical models, but that the operational consumer must recognize the sources of error and the inherent uncertainties of any predicted fallout pattern.

The classification of RM-2334 is CONFIDENTIAL–FORMERLY RESTRICTED DATA; the classification of this abstract is CONFIDENTIAL.

CONFIDENTIAL

CONFIDENTIAL

The RAND Corporation, Santa Monica, Calif.
USAF Project RAND RM-2334

SUMMARY REPORT OF RAND WORK ON THE AFSWP FALLOUT PROJECT (U) by R. R. Rapp; Research Memorandum RM-2334, February 25, 1959, CONFIDENTIAL–FORMERLY RESTRICTED DATA. 73 pp. incl. illus.

A concluding study of an investigation dealing with the physical processes of local radioactive fallout caused by surface-burst nuclear weapons, and with the development of mathematical models that would permit the computation or prediction of surface fallout patterns. This summary discusses the basic parameters needed to construct a fallout computation model, considers the relative importance, availability, and accuracy of the inputs to the model, describes the various RAND fallout models, and evaluates fallout models generally as operationally useful prediction devices. It is concluded that reasonably accurate fallout forecasts are possible through the use of mathematical models, but that the operational consumer must recognize the sources of error and the inherent uncertainties of any predicted fallout pattern.

The classification of RM-2334 is CONFIDENTIAL–FORMERLY RESTRICTED DATA; the classification of this abstract is CONFIDENTIAL.

CONFIDENTIAL

The RAND Corporation, Santa Monica, Calif.
USAF Project RAND RM-2334

SUMMARY REPORT OF RAND WORK ON THE AFSWP FALLOUT PROJECT (U) by R. R. Rapp; Research Memorandum RM-2334, February 25, 1959, CONFIDENTIAL–FORMERLY RESTRICTED DATA. 73 pp. incl. illus.

A concluding study of an investigation dealing with the physical processes of local radioactive fallout caused by surface-burst nuclear weapons, and with the development of mathematical models that would permit the computation or prediction of surface fallout patterns. This summary discusses the basic parameters needed to construct a fallout computation model, considers the relative importance, availability, and accuracy of the inputs to the model, describes the various RAND fallout models, and evaluates fallout models generally as operationally useful prediction devices. It is concluded that reasonably accurate fallout forecasts are possible through the use of mathematical models, but that the operational consumer must recognize the sources of error and the inherent uncertainties of any predicted fallout pattern.

The classification of RM-2334 is CONFIDENTIAL–FORMERLY RESTRICTED DATA; the classification of this abstract is CONFIDENTIAL.

CONFIDENTIAL

Copy No. 32

RAND RESEARCH MEMORANDUM

SUMMARY REPORT OF RAND WORK ON THE AFSWP FALLOUT PROJECT (U)

R. R. Rapp

RM-2334 February 25, 1959

in brief

Operations analysts and radiological-weapons-effects people will be interested in this concluding report of a study sponsored by the Armed Forces Special Weapons Project, now the Defense Atomic Support Agency. The investigation considers the physical processes of local radioactive fallout caused by surface-burst nuclear weapons and the development of mathematical models that would permit the computation or prediction of surface fallout patterns. (Research memorandums RM-1932, RM-2006, RM-2108, RM-2115, RM-2148, RM-2193, and RM-2296, and Classified Paper S-62 are part of this series. The basic mechanisms for understanding local fallout are also investigated in R-309, Close-in Fallout.)

In particular, this summary discusses the basic parameters needed to construct a fallout computation model. The parameters examined are the distribution of activity with particle size, the distribution of the activity in space at the time of stabilization, the fall velocity of the particles, and the wind structure. The study considers the relative importance, availability, and accuracy of the inputs to the model, describes the various RAND fallout models, and evaluates fallout models generally as operationally useful predicition devices.

It is concluded that reasonably accurate fallout forecasts are possible through the use of mathematical models, but that the operational consumer must recognize the sources of error and the inherent uncertainties of any predicted fallout pattern.

CONFIDENTIAL

The RAND Corporation
1700 Main St. • Santa Monica • California

DEFENSE THREAT REDUCTION AGENCY
Defense Threat Reduction Information Analysis Center (DTRIAC)
1680 TEXAS STREET SE
KIRTLAND AFB, NM 87117-5669

BQ (505) 846-1775

12 July 2006

To: Larry Downing, DTIC

Subject: Declassification/Distribution Review

Per DTRA Review:

AD 352651
Fallout Intensities and Shielding Factors (For Use With Nuclear Weapons Employment constraints), DASA Staff Study (U) DASA 617

- **Report remains SRD, with Distribution Statement C assigned.**

AD 860198
Simulation Techniques for Composite Shield Testing, Pt. 2, Short Pulse Width (1 to 2 msec) Energy Releases and Energy Profiling in Uranium Loaded Test Specimens Using Triga (U) DASA 2343-2

- **Report remains Unclassified with Distribution Statement C assigned.**

AD 337920
Summary Report of Rand Work on the AFSWP Fallout Project (U) AFSWP-1134.

- **Report Declassified and Distribution Statement A assigned.**

Darlene Rosales

Darlene Rosales
COTR,
Defense Threat Reduction Information
Analysis Center (DTRIAC)